ELECTRIC FIELD AND PRESSURE ENHANCED MAGNETIC PROPERTIES OF MULTIFERROIC MATERIALS AND BiFeO_3, AND ENHANCEMENT OF CRITICAL TEMPERATURE OF SUPERCONDUCTOR(SmAsFeOF) UNDER PRESSURE

A Dissertation Submitted to the Department of Physics, Addis Ababa University

In Partial Fulfilment of the Requirement of the Degree of Doctor of Philosophy in Physics

Department of Physics

Addis Ababa University

Abera Mebrahtu

Addis Ababa, Ethiopia, March 13, 2018

DECLARATION

I hereby declare that this PhD dissertation is my original work and has not been presented for a degree in any other university, and that all sources of material used for the dissertation have been duly acknowledged.

Name: Abera Mebrahtu

Signature: ——————

This PhD dissertation has been submitted for examination with my approval as university advisor.

Name: Prof P. Singh

Signature: ——————

Place and date of submission:

Addis Ababa University

Department of Physics

March, 2018

Addis Ababa University
Department of Physics

This is to certify that the dissertation prepared by Abera Mebrahtu Abraha, entitled ELECTRIC FIELD AND PRESSURE ENHANCED MAGNETIC PROPERTIES OF MULTIFERROIC MATERIALS AND $BiFeO_3$, AND ENHANCEMENT OF CRITICAL TEMPERATURE OF SUPERCONDUCTOR($SmAsFeOF$) UNDER PRESSURE submitted in fulfillment of the requirements for the degree of Doctor of Philosophy(Physics) complies with the regulations of the university and meets the accepted standards with respect to originality and quality.

Professor. Rajeev Ahuja, External Examiner _____

Dr. Chernet Amentie, Internal Examiner _____

Professor Pooran Singh, Advisor _____

Dr. Teshome Senbeta, Chairman _____

Dated: March 13, 2018

Contents

List of Figures

Acknowledgements

Above all, I would like to thank the almighty God who help me to accomplish this work. Next, I would like to express my sincere thanks to my advisor and instructor Prof. P. Singh, for his unlimitted guidance, assistance, supervision and contribution of valuable suggestions through out my study, and I would like to direct special thanks to Prof. Rajeev Ahuja for offering me to visit his research group and for his permission and support to use VASP license, cloud computers and other facilities in Uppsala University, Department of Astronomy and Physics during my stay. I would further thank to Abduselam International center for theoretical Physics staff of Trieste, who introduced me Quantum Espresso, professional software. I acknowledge the financial support of Addis Ababa University Graduate office, Gondar University(my Sponser University).

I am grateful to Dr. Teshome, chairman of the department, w/r Tsilate, secretary of the department, Dr. Belayneh, the former chairman of the department of Physics, AAU, for their help through out my contact with the department. I appreciate the support from the staff at AAU and GU.

I would like to thank every one in particular, Dr. Sudip, vivek, Rafel, Rubab and others, for their support while I was a visiting student at Uppsala University. Finally, I would like to express thanks from bottom of my heart to all my parents and family members, for their love, and continues support.

Abstract

In this dissertation we have studied electric field enhanced magnetic properties of multiferroic materials . The system contains a ferromagnetic and a ferroelectric sub lattices. To describe the property of system, we considered linear coupling Hamiltonian between ferromagnetism and ferroelectricity without microscopic derivation. The thermodynamic properties of the system are calculated, such as magnon excitation spectrum , temperature dependences of magnetization, internal energy, specific heat capacity, and magnetic susceptibility subjected to electric and magnetic fields. In addition to this electronic and structural properties of multiferroic material(BiFeO_3) are studied using density functional theory. We also investigate critical temperature of iron based superconductors (SmAsFeOF) under the influence of an external hydrostatic pressure based on density functional theory calculations using Vasp and quantum Espresso Code coupled with Migdal Eliashberg model. Our results show that the critical temperature increases up to 45.91K under the pressure upto 30GPa and, subsequently, drops down until 60GPa. Throughout this pressure range, the system is preserving the initial symmetry without any structural transformation. Our results indicate that the enhancement of critical temperature is due to increase electron boson (phonon/spin fluctuation) coupling and further increase of pressure may lead to instability of system. Our theoretical results are in agreement with the experiments.

1

INTRODUCTION

In the past few years there has been a revival of interest in multiferroics materials, in which electric and magnetic ordering coexist. Multiferroics are considered now as promising materials for magnetic storage, spintronics devices and microwave technique as they provide a novel approach to the magnetic field or electric field conversion. The coupling of magnetic and electric subsystems results in magneto electric (ME) effect (linear ME effect), i.e. the electric field induced magnetization and magnetic field induced electric polarization.

In these materials magnetism and ferroelectric ordering coexist no matter how their course of existence varies from material to material [1]. The microscopic description of magnetism is based on the localized magnetic moments, mostly due to the partially filled d or f shell of transition metal or rare earth elements electrons in which the exchange interactions between these localized moments exhibit magnetic orderings. The origin of ferroelectrics is wide range (can be due to: Charge ordering, lone pairs) and forbids the d shell electrons in contrast to magnetism [2, 3]. They remarkably show strong coupling between charges, spins, lattice and orbital degrees of freedom and the interplay between various competing orders gives rise to interesting features and varieties to these classes of materials. The overlap of strongly correlated magnetic and ferroelectric orders enable one domain over the

other [4–6]. For instance, in ferromagnetic materials the magnetization M is easily switchable parameter on an application of external stimulating magnetic field, H and in ferroelectrics the polarization P is also a controllable parameter by an external electric field, E. However, in multiferroics these switchable order parameters, P and M are cross linked, i.e. magnetization can be switched by external electric field and polarization can also be tunned by an applied magnetic field [7, 8].

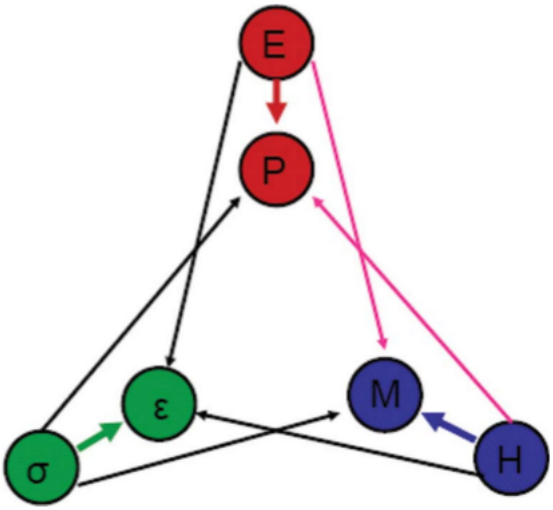

Fig. 1.1: Possible cross couplings in multiferroics. E electric field; P electric polarization; σ applied mechanical stress; ε strain; H magnetic field; M magnetization [8].

The already known or synthesized multiferroics displayed very small magnetoelectric coupling effect and usually this was manifested only at very small temperatures. These features made mutiferroics nothing more than an interesting subject for academic research, since most useful applications require room temperature operation and large magnetoelectric coupling. Moreover, this was complemented by a limited understanding of the microscopic nature of multiferroicity and magnetoelectric coupling, which led unsurprisingly to a decline in multiferroics research activities for almost 20 years. [9–12].

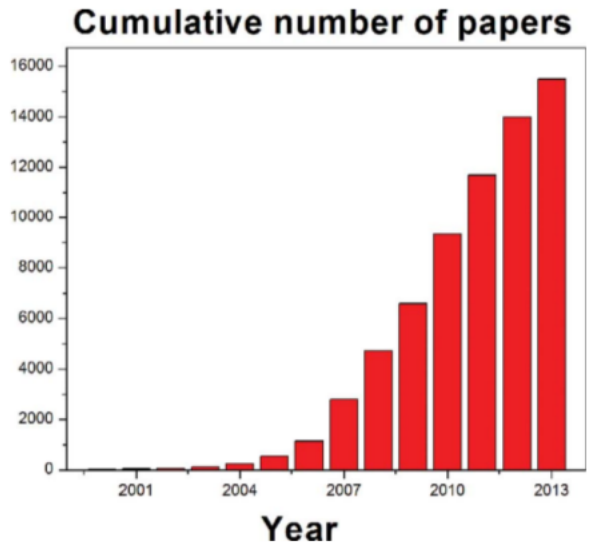

Fig. 1.2: Cumulative number of published articles searched using the keyword multiferroic in Google Scholar. The data covers the period 2000 - 2013 [12]

The theoretical backgrounds and experimental efforts helped the field to envisage fast, huge memory and multifunctional devices in the electronics industry. Prominently, in the spintronics world where the spin and the charge degrees of freedom play independent roles so as to manipulate spin and electronic properties separately. These features of the composite multiferroics can be considered as an exclusive means to point out the coexistence of coupled order parameters. The existence of simultaneous order parameters in some naturally occurring compounds is very weak to be used in wide ranges of applications and also very rare due to several constraints. The comparatively few number of single phase(naturally found) multiferroics put sever limitations to the researchers not to proceed further on the same track. However, the possibility of the coupled order parameters in synthesized compounds of different strengths have triggered the spirit onto composite ferroelectric-ferromagnetic multiferroics providing magnetically ordered phases and electrically active states besides the elastic responses. Such composites have rich phase dia-

grams, not only because they have the properties of their parent compounds, but also interactions between the magnetic and electric orders lead to additional functionalities such as the four state logic devices [14]. The general principle underlying on the quantum mechanical description of the interacting particles with the surrounding environment is on the pursuit of small perturbation that leads to elementary excitations. In the composite systems of FE, FM nano structured materials, coupling is inevitable so long as there is magneto(electro) striction effects that can be shared from one component to the other and, consequently, modifies the magnetizations and polarizations of the system. The physics of these materials is full of surprises and undoubtedly gives rise to challenging phenomena at this time and in the future the new science of multiferroics will certainly spark out if concerted efforts brought together.

The literature survey, theoretical procedure for system and results and discussion of research work have been organised into seven chapters of this thesis. Chapter wise discussions are given below:

Outlines of the thesis

Chapter 1: This chapter contains the overall introduction of the thesis.

Chapter 2: This chapter contains a brief introduction of, ferroelectricity, magnetism and multiferrocity. The origin and history have been discussed. In addition to this, recent developments and motivation to carry out research ,basic principles of theory of magnetoelectric and multiferroic materials are explained. We first discuss a phenomenological approach to the magnetoelectric effect, and then turn to the microscopic mechanisms that give rise to ferroelectricity in frustrated magnets where competing interactions between spins result in states without inversion symmetry.

Chapter 3: A theoretical model Hamiltonian is set considering for multiferroic materials that can be described making use of the magnon operators which represents strongly correlated systems of multiferroics and is treated theoretically using the double time Greens Function.

Chapter4: We consider the First Priciple Theory or Density Functional Theory(DFT) using VASP code to describe electronic and structural properties multiferroic (**BiFeO3**).

Chapter 5: Focus High Pressure driven Superconducting critical temprature in Iron based Superconductivity (**SmAsFeOF**) applying Density Functional Theory(DFT) using VASP and Quantm espresso code.

In the last two chapters we look at Results and Discussions, and the executive summary of the whole work and the findings are presented accordingly with the contention of experimental results.

2

Ferroelectricity

The ferroelectric effect was discovered in 1920 by Joseph Valasek, who obtained hysteresis curves for Rochelle salt analogous to the hysteresis curves of ferromagnetism [14]. In March 1935 potassium dihydrogen phosphate (KDP), KH2PO4 was found to be ferroelectric with a critical temperature of about 123 K by Busch and Scherer [15] where its isomorphs also contains the properties of ferroelectricity. The first phenomenological theory was proposed in 1940 by Muller to describe the relations between piezoelectric, anomalous dielectric and elastic behaviors of Rochelle salt. In 1941, Slater introduced the first significant microscopic theory of phase transitions based on the model of hydrogen bonds to explain the behavior of KH2PO4. After 1941, the third major ferroelectric substance, barium titanate $BaTiO_3$, was discovered [16]. Barium titanate was the first man made perovskite ferroelectric material in ceramic form. In the following years several isomorphs of $BaTiO_3$ were found to behave also as ferroelectrics. In 1949, Devonshire published a theory on the phase transition mechanism of $BaTiO_3$ [17]. His theory has deepened the understanding on the behavior of $BaTiO_3$ and has initiated the thermodynamic theory in ferroelectricity. A major breakthrough in the study of ferroelectricity came from Cochran [18] and Anderson [19] via the soft modes description of ferroelectricity in the perovskite. The development of the ferroelectric soft mode theory occupied the

duration from 1959 to 1970. From 1980 until now, many ferroelectrics have been discovered and research activity has rapidly increased.

Ferroelectrics are a special class of piezoelectric materials(Converts Mechanical energy into electrical energy) have been widely used as transducers. They exhibit a spontaneous polarization that can be reversed or swiched (by application of stress or electric field). They are very attractive because of their switchable polarizations.

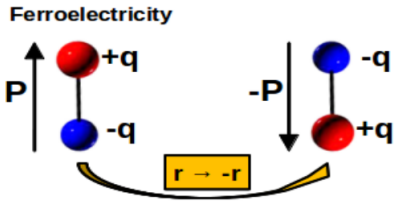

Fig. 2.1: polarization swiches from minus to positive charge [18]

There are pre existing dipoles in these materials even in the absence of external electric field. They originate from the minor deviation from crystallographic symmetry of the materials. dipoles are aligned along the field lines in case of the orientation polarization. Typically, materials demonstrate ferroelectricity below the Curie temperature, T_c.

Dielectric materials are grouped according to the reaction of the polar constituents on an external electric field. This electric field induces a displacement of electrons and ions with respect to the field free position. In case of induced polarization the center of charges coincide, whereas an external electric field shifts of the center of charge and induces a polarization. Ferroelectric (FE) materials are characterized by a reversible spontaneous macroscopic polarization which is the electric dipole moment per unit volume. By applying an external electric field the direction of the polarization can be reversed. These dipoles upon reconfiguration into small regions of different states each with random polarization directions undergoing structural

phase transition determines the macroscopic electrical properties of the crystal.

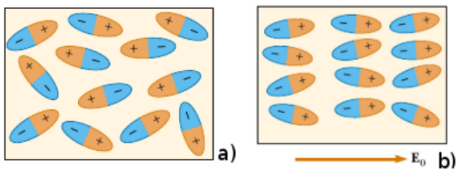

Fig. 2.2: The above illustrations indicate the polarization in dielectric crystal. In a) the dipoles in the polar crystals are randomly oriented. But if an external field E_o , is applied these dipoles align themselves in the direction of the field as shown in figure b [19].

The most prominent features of ferroelectric properties are hysteresis and non-linearity in the relation between the polarization P and the applied electric field E. Dielectric materials exhibit a linear relationship between polarization and electric field. On the other hand, paraelectric materials, show a more enhanced non linear dependence.

In this case, the slope of the polarization curve which represents the electric permittivity is not constant as in dielectrics but is a function of the external electric field. These features are shown below. The coercive field E_c denotes the critical electric field, required to reduce the polarization to zero after the polarization of the sample has been driven to saturation region. Due to the unique combination of these properties researchers and engineers have been focusing on ferroelectric materials application in electronic devices such as sensors, infrared detectors, microwave phase and filters.

2.1 Mechanisms for ferroelectricity in multiferroics

A necessary but not sufficient condition for the appearance of spontaneous electric polarization is the absence of inversion symmetry. We can distinguish between

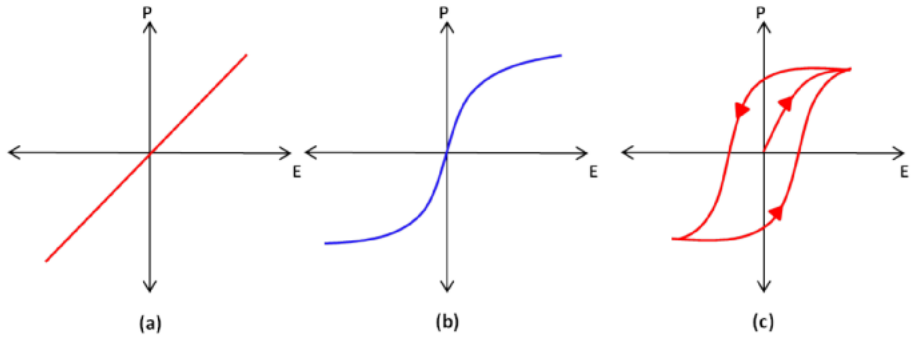

Fig. 2.3: Schematic hysteresis loop of the electric field dependency of the (a) Dielectric polarization, (b) Paraelectric polarization, (c) Ferroelectric polarization [20].

proper and improper ferroelectric (FE). The difference lies in the driving force (the primary order parameter) that leads to ferroelectricity: In the case of proper FE, the primary order parameter is the ferroelectric distortion. One example of proper FE is $BaTiO_3$ where a covalent bonding between the transition metal and the Oxygen happens to allow a polar state. In usual perovskite based ferroelectrics like $BaTiO_3$, the ferroelectric distortion occurs due to the displacement of B-site cation (Ti) with respect to the Oxygen octahedral cage. Here the transition metal ion (Ti in BaTiO3) requires an empty d shell since the ferroelectric displacement occurs due to the hopping of electrons between Ti d and O p atoms. For technological applications its highly desirable to combine ferroelectric and ferromagnetic order within one material [20].

2.2 Magnetism

Let discuss the behavior of the spins, as a function of temperature, in materials described by the Heisenberg model. At high temperatures there are strong thermal fluctuations so that the spins are disordered, meaning that the expectation value of each spin vanishes: $< S_i >$ = 0. (Here the brackets represent both a thermal

and quantum mechanical expectation value.) However, below some critical temperature T_c it may be that the spins order magnetically, meaning that the spins on average point in some definite direction in spin space, $< S_i \geq 0$. Whether or not such magnetic order occurs depends on the dimensionality and type of lattice, and the range of the interactions (we will limit ourselves to hypercubic lattices and nearest neighbor interactions in our explicit investigation of the Heisenberg model). If magnetic order occurs with $T_c > 0$, then, as the temperature is lowered from T_c down to zero, S_i will increase and reach some maximum value at zero temperature. The critical temperature T_c is called the Curie temperature (T_c) in ferromagnets and the Neel temperature (T_N) in antiferromagnets.

The occurrence of magnetism in transition metal oxides is mainly due to the magnetic moments of the electrons in the partially filled shells. The non zero spin angular momentum associated with an unpaired electron, an electron that occupies an orbital of an atom singly rather than as part of an electron pair, gives rises to a magnetic moment. Ferromagnetic materials like transition metals, exhibit parallel alignment of magnetic moments to one another giving net spontaneous magnetization even in the zero magnetic field. In an antiferromagnet, equal magnetic spins are aligned antiparallel, as a result the material shows no net magnetic moment. Transition metal oxides are a good examples of AFM materials. Ferrimagnetism is a special case of antiferromagnetism, consisting antiparallel unequal moments, resulting in a non zero net magnetization. This behavior is observed in complex salts of the transition elements like MnO or Fe2O3 [21].

Depending on the magnetic properties materials are classified as diamagnetic, paramagnetic, ferro(antiferro)magnetic, and ferrimagnetic. In some materials, such as diamagnetics and paramagnetics, the induced magnetization is proportional to

the applied field whereas in others, nonlinear relations exist as characterized by the hysteresis curves. In some crystalline materials permanent dipole moments are there and found to be in the form of microscopic regions within which all moments align in the same direction. Thus, if weak external field is applied, these dipoles remain aligned to give rise to the macroscopic ferromagnetic character of the crystal even after the removal of applied field. Some of the examples of elements that show spontaneous magnetization or in other words exhibiting ferromagnetism are: The transition or iron group elements (e.g. Fe, Ni, Co), the rare earth group elements (e.g. Gd or Dy), and many compounds and alloys that are the play grounds for research and investigation purposes.

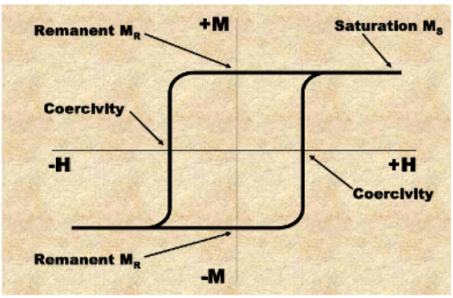

Fig. 2.4: The above illustration shows the magnetic hysteresis curve of the ferromagnetic material [21].

2.3 Exchange interaction

There are several origins for the interactions between the magnetic moments that can lead to a long range ordering of the unpaired spins, called exchange interactions. For spontaneous magnetization electron electron interaction is a must. The rare earth metals Gd, Dy, and the insulating transition metal oxide CrO2 all becomes ferromagnetic under suitable circumstances. The phenomena is restricted to transition and rare earth elements and is related to the unfilled 3d and 4f shells in these

substances.

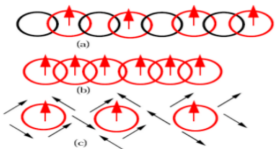

Fig. 2.5: Schematic illustration of a) super exchange. where the interaction takes place via an intermediate non magnetic ion; and (b) direct exchange, in which the magnetic ions interact through their overlapping charge distributions; ((c) indirect exchange, in which the interaction is mediated by interactions with the charge carriers

2.4 Magnetic Frustration

In a square lattice, the system can easily find an ordered structure of spins to satisfy antiferromagnetism. In some other materials, where the free spins are arranged in a triangular or tetrahedral pattern, there is no way to simultaneously satisfy all of the magnetic interactions. In these materials, magnetic order is said to be frustrated. Frustration occurs when there is no possible spin configuration that can satisfy a number of competing exchange interactions and minimize the ground state energy. Only two out of the three spins can align antiparallel, the third spin lacks a preferred direction along which to point because of competing interactions with its neighbors. Unlike the cases of ferromagnetism and antiferromagnetism, in frustrated materials, the minimum energy state may be composed of magnetic moments arranged in a more complex pattern, such as repeating spirals (helimagnetism), frozen into random orientations with no long range order as in spin glasses, or form an incommensurate order. Alternatively, there may be an enormous number of equally favorable ground states, so that no particular state stabilizes and the

magnetic moments freely fluctuate down to the temperatures available in the laboratory (spin liquid). It also could be the case that magnetic order only achieved at extremely low temperatures due to some symmetry breaking transition as in spin ice.

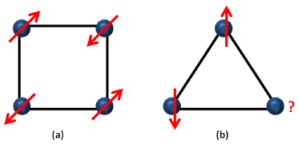

Fig. 2.6: (a) Anti parallel alignment of the magnetic moments in a square lattice and (b) Frustration of magnetic order in triangular lattice.

2.5 Definition of Multiferroics

Multiferroic materials are a kind of compound, and in each of them the magnetic and electric orders coexist below a certain temperature. The interaction between the two types of orders, called magnetoelectric (ME) coupling, yields some additional features to the ferroelectric and magnetic transitions and introduces possible multifunctional responses to an external electric or magnetic field [22–24]. Because of the interaction between the two kinds of orders in such materials,i.e. the magnetoelectric coupling, the magnetic properties could be changed by the ferroelectric ordering or an external electric field, and the electric properties can also be changed by the fluctuation of spin ordering or an external magnetic field. The effect of magnetoelectric coupling is particularly strong when temperature is close to or just below magnetic phase transition temperature and may result in a change of electric properties [25–27].

The mutual effect between the magnetic and electric orders makes these compounds ideal for applications in information storage, in the emerging field of spin-

tronics, and sensors. [28]

2.6 History of Multiferroics

After the first observation of magnetoelectric effect by Rontgen in 1888 subsequent progressive investigations have been made and found to trigger research activities. Particularly, around 1960,experimental endeavors successfully ensure the magnetoelectric effect, inspite of being the coupling strength of the apparently different properties was very small in magnitude. The experimental result obtained on Cr2O3 has twinkled a spirit of attention on various materials exhibiting this extraordinary effect that can attribute for practical applications and also remarkably for fundamental understanding from theoretical view points. This new emerging science has opened a new route towards the magnetoelectric switching on the expense of the cross coupling of the polarization and magnetization parameters. The progress on the field, later showed some more materials such as Ti_2O_3 , Boracites, phosphates, Ba,Bi,and Ga ferrites, perovskites and others. The research interest in the 1960 and 1970 was so hot, and gradually went down till the 1990. However, a resurgence comes on while the field of study, multiferroism with new terminology evolves out. The field of multiferroics is strongly tied with the birth of magnetoelectrics and has passed ups and downs too. For the success of multiferroics growth different scenarios have been forwarded. Of the most remarkable reasons, the rareness of materials with coexisting of magnetoelectric coupling and in the absence of ferroelectricity in magnetic systems, the theory of the induction on the expense of magnetism take the lead [29,30]. The term Multiferroic was coined by H.Schamid in 1994 for the first time and served till today. Although considerable motivations and an initial burst of interest arose until 2000, research in the field remains some how static due to

material specific reasons. However, in 2003 very great discoveries reenforced the renaissance of the multiferroic studies. The first one is the discovery of most popular multiferroics thin film, $BiFeO_3$ with an enhanced coupling particularly in thin film form better than the bulk sample [31]. The second and third belongs to the experimental investigation of the novel class of multiferroics, in which the the magnetic and ferroelectric properties do not coexist, but magnetism can lead to ferroelectricity and hence coupling is possibly true. Magnetically induced polarization is, of course, very small so as to be used for practical applications, but opened new route towards another way of multiferroism. This surmountable evidence was observed in compounds of $TbMnO_3$ by Tokura and Kimura and latter on, a similar effect was confirmed on $TbMn_2O_5$ by another researcher, Cheong [32,33]. The first ever found multiferroic material with simultaneous ferroelctric and ferromagnetic coupled ordered states was Nickel Iodine boracite $Ni_3B_7O_{13}I$. Subsequently, while research was carried on various materials have been found with coupled ordered states.

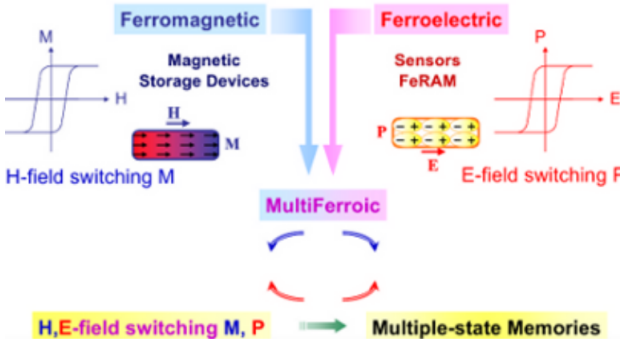

Fig. 2.7: The illustration shows very common primary ferroic orders in multiferroics accessible for switching of multistate functionalities [34].

2.7 MAGNETOELECTRIC EFFECT

Multiferroic materials are interesting not only because they exhibit ferroelectric and magnetic properties but also due to the magnetoelectric effect, by which an induced electrical polarization and magnetization can be controlled by applying a magnetic and electric field, respectively.

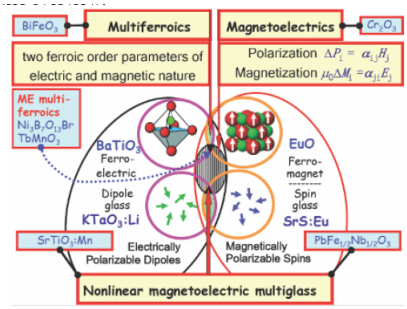

Fig. 2.8: The world of electrically and magnetically polarizable materials including bare ferroics, multiferroics, linear magnetoelectrics [35], and dipole, spin, and nonlinear ME multiglasses [36–38].

$$\frac{dP}{dH} = \alpha_H \tag{2.1}$$

and

$$\frac{dM}{dE} = \alpha_E \tag{2.2}$$

Where α_H and α_E are induced magnetization cofficient and induced polarization cofficient respectively. This effect can potentially be exploited to allow the construction of novel spintronic devices such as tunneling magnetoresistance (TMR) sensors, spin valves with functionality that is tunable by an electric field, and multistate memories in which data are written electrically and read magnetically. However, in order to be useful for applications, the magnetoelectric coupling must be both large and active at room temperature. Multiferroics may be classified due to

the mechanism leading to the appearance of both order parameters. This interaction between the electrical properties and magnetization makes this material very important in a variety of applications. These materials can be single phase (direct magnetoelectric effect coupling) or multiphase coupling (strain mediated magnetoelectric coupling). Electric and and magnetic orders are related by the following equations respectively,

$$P = X_e E$$

$$M = X_m H$$

Where X_e and X_m are dielectric and magnetic susceptibility of the materials respectively. The single multiferroic ordering with direct ME coupling is given by,

$$P = X_e E + \alpha_m H \tag{2.3}$$

$$M = \alpha_m H + X_e E \tag{2.4}$$

The multiphase multiferrioc ordering with strain mediated ME coupling is also given by

$$P = X_e E + \alpha_m H + \pi\alpha H \tag{2.5}$$

$$M = X_m H + \alpha_e E + \pi\sigma H \tag{2.6}$$

As stated above, ferroelectric perovskite oxides need B-site TM ions with an empty d shell to form ligand hybridization with the surrounding anions. This type of electronic structure likely excludes magnetism. However, not all experimental and theoretical results support the argument that ferroelectricity and magnetism are absolutely incompatible, and an integration of them seems to be possible. First, the

famous Maxwell equations governing the dynamics of electric field, magnetic field and electric charges, tell us that rather than being two independent phenomena, electric and magnetic fields are intrinsically and tightly coupled to each other.

A varying magnetic field produces an electric field, whereas electric current, or a charge motion, generates a magnetic field. Second, the formal equivalence of the equations governing the electrostatics and magnetostatics in polarizable media explains the numerous similarities in the physics of ferroelectricity and ferromagnetism, such as their hysteresis behavior in response to the external field, anomalies at the critical temperature and domain structures. On the one hand, these coupling phenomena and similarities in terms of the electric dipoles and spins in polarizable media imply the potential to integrate ferroelectricity and magnetism into single phase materials.

According to Landau theory, the Gibbs free energy for magnetoelectric system can be written as

$$G(E,H) = G_0 - P_i^s E_i - M_i^s H_i - \frac{1}{2}\varepsilon_0\varepsilon_{ij}E_iE_j - \frac{1}{2}\mu_0\mu_{ij}H_iH_j$$

$$- \alpha_{ij}E_iH_j - \frac{1}{2}\beta_{ijk}E_iH_jH_k - \frac{1}{2}\gamma_{ijk}H_iE_jE_k \tag{2.7}$$

where G_0 is the ground state free energy, subscripts (i, j, k) refer to the three components of a variable in spatial coordinates, E_i and H_i are the components of the electric field E and magnetic field H, respectively, P_i^s and M_i^s are the components of spontaneous polarization P^s and magnetization M^s , ε_0 and μ_0 are the dielectric permeability and magnetic susceptibility of vacuum, ε_{ij} and μ_{ij} are the second order tensors of dielectric permeability and magnetic susceptibility, β_{ijk} and γ_{ijk} are the thirdorder tensor coefficients and, most importantly, a α_{ij} is the component of a tensor which is designated as the linear magnetoelectric effect and corresponds to

the induction of a polarization by a magnetic field or a magnetization by an electric field [39].

The polarizations and magnetizations are obtained upon differentiating the free energy with respect to the fields.

The polarization is given by

$$P_i(E,H) = -\frac{dG}{dE_i} = P_i^s + \varepsilon_0\varepsilon_{ij}E_j + \alpha_{ij}H_j + \frac{1}{2}\beta_{ijk}H_jH_k + \gamma_{ijk}H_iE_j \tag{2.8}$$

and magnetization also given by

$$M_i(E,H) = -\frac{dG}{dH_i} = M_i^s + \mu_0\mu_{ij}H_j + \alpha_{ij}E_j + \beta_{ijk}E_IH_J + \frac{1}{2}\gamma_{ijk}E_JE_K \tag{2.9}$$

The tensor α corresponds to induction of polarization by a magnetic field or of magnetization by an electric field which is termed as the linear ME effect. For instance, it can only be nonzero for materials that simultaneously break time reversal symmetry and spatial inversion symmetry. The most common source of time asymmetry in Mott insulators is spin ordering. The magnetoelectric coupling appears if the spin ordering breaks inversion symmetry. The components of the linear electromagnetic coupling parameter are constrained by thermodynamics stability criteria and is bounded by an appropriate diagonal elements of dielectric permittivity and magnetic permeability parameters related to

$$\alpha_{ij} = \frac{\sqrt{\varepsilon_{ii}\mu_{jj}}}{4\pi}$$

It is supplemented by higher order ME effects, nonlinear ME susceptibilities like those parametrized by the tensors β and γ. These linear and non linear magnetoelectric susceptibility parameters characterize the performance of magnetoelectric

materials. In most cases, interest arises to know about the linear magnetoelectric coefficient, as magnetoelectric effect is linear in most compounds. This coefficient basically quantifies the dependence of polarization on magnetic field or of magnetization on the electric field. In case of multiferroics, although many linear magnetoelectric effects are expected because these materials often possess large susceptibility and permeability respectively. The values of ME coupling parameter for single phase material has always been found to be very small, on the order of several $\frac{mV}{cm}$. This small ME effect makes it hard for them to be useful for devices applications. However, more recent investigations have been reported that improved multiferroic and ME properties in epitaxial layers of ME thin films such as $BiFeO_3$ grown on $SrTiO_3$, and in self assembled multiferroic nanostructures such as $CoFe_2O_4$ nanopillars embedded in a $BaTiO_3$ matrix on $SrTiO_3$ substrates can exhibit better enhancement and potentially useful for integrated microelectronic materials that have the promise of reading a spin state as a direct voltage. Unfortunately, the electronic configurations which favor polarization are antagonistic to those that favor magnetization, and vice versa. This is simple to conceptualize, i.e, the d^n electronic configuration is favorable to spin alignment, but is not very distortable; whereas d^0 is very distortable, but has no spin. ME effect involves both magnetic and electric properties and hence it seems hard to maintain both space time symmetric operations, consequently leading to complexity on the behaviors of the materials.

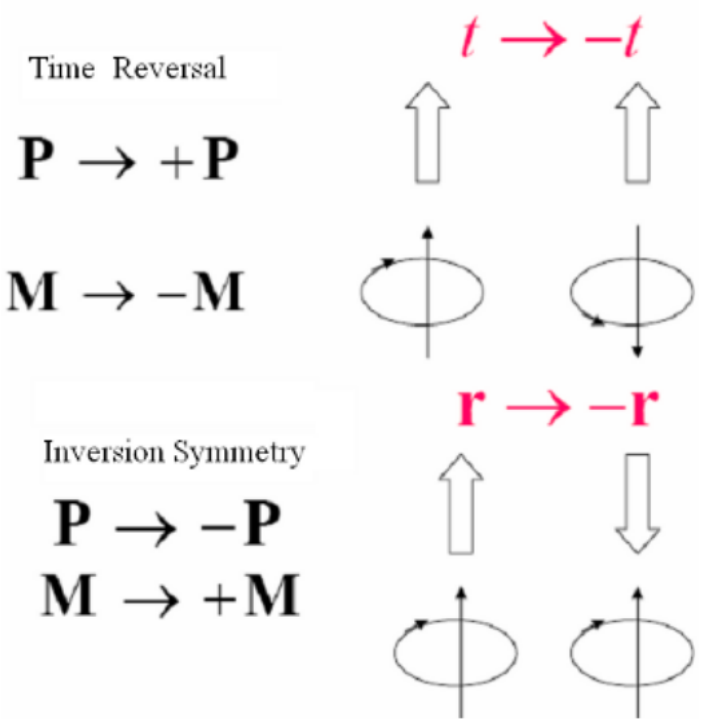

Fig. 2.9: The violation of time and space symmetry while both ferroelectric and ferromagnetics are combined in to one component.

3

Formulation of the problem

3.1 Model and method

In this work, a simplest construction is assumed. The Hamiltonian of the system with external electric field E and magnetic field H can be expressed as [40–45].

$$H = -\sum_{i,j} J_{ij} S_i . S_j - g\mu_B H \sum_i (S - n_i) + D \sum_i (S^2 - n_i)$$
$$- \mu_E \sum_i (S - n_i) + \lambda \sum_i S_i^z . \sigma_i^z \tag{3.1}$$

Where S_i S_j is spin operator at sites i(j), J_{ij} is the exchange coupling that depends on the relative positions of neigbhoring spins and is defined by J_{ij} = $J(R_i - R_j)$. The constant g is the gyromagnetic ratio, and the second term of Equation (1) is the effective Zeeman field with an external deriving field while in this model chosen to be parallel to the +z axis to line up all the spins in the same direction. Whereas, the fourth term includes an electric field E that interacts with the spins in the system. The constant μ describes the coupling strength between the spins and the radiation field. The terms μ_B and D are the Bohr magneton and magnetic anisotropic (or spin wave stiffness) constants,respectively. And the last term describes the interaction between localized magnetic moment S_i^z and the itinerant electrons σ_i^z, where λ is the corresponding exchange coupling constant. Where $S_i.S_j$, S_i^z, and S_j^z are spin devation operators at site (ijk) respectively, and expressed as

$$S_i.S_j = \frac{S_i^+ S_j^- + S_i^- S_j^+}{2} + S_i^z S_j^z$$

$$S_i^z = S - n_i$$

$$S_j^z = n_j - S$$

Transforming the spin ladder operator problems in to many body interaction systems, bosonic creation and annihilation operators expressed as,

$$S_i^+ = \sqrt{2s}(1 - \frac{a_i^+ a_i}{2s})^{\frac{1}{2}} a_i \tag{3.2}$$

$$S_i^- = \sqrt{2s} a_i^+ (1 - \frac{a_i^+ a_i}{2s})^{\frac{1}{2}} \tag{3.3}$$

Where a_i^+ and a_i are the creation and annihilation spin devation operators satisfying the commutation relation $[a_i, a_i^+] = 1$.

It is possible to transform this bosonic operators to magnon variable operators to a_k and a_k^+ in the low temperature limit.

$$a_k = \frac{1}{\sqrt{N}} \sum_i e^{ik.x_i} a_i \tag{3.4}$$

$$a_k^+ = \frac{1}{\sqrt{N}} \sum_i e^{-ik.x_i} a_i^+ \tag{3.5}$$

Where the inverse transformation is

$$a_i = \frac{1}{\sqrt{N}} \sum_k e^{-ik.x_i} a_k \tag{3.6}$$

$$a_i^+ = \frac{1}{\sqrt{N}} \sum_k e^{ik.x_i} a_k^+ \tag{3.7}$$

And spin density of conduction electrons is also given by

$$\sigma^{z}_{k,q} = c^{+}_{k\uparrow}c_{k\uparrow} - c^{+}_{k+q\downarrow}c_{k+q\downarrow} \tag{3.8}$$

Where k is wave vector and q is a momentum vector, restricting the involved momentum in the first Brilloun zone and fourier transforming the fermionic and bosonic operators, and considering only predominated bilinear spin variables, the total Hamiltonian is written in the second quantized form as

$$H = (\beta k^2 - 2DS + g\mu_B H + \mu E)\sum_{k}^{N} a^{+}_{k\uparrow}a_{k\uparrow} + JS\sum_{k,q}^{N} a^{+}_{k-q\downarrow}a_{k-q\downarrow}$$

$$+\frac{\lambda s}{N}\sum_{k,q}^{N} a^{+}_{k\uparrow}a_{k\uparrow}(C^{+}_{k\uparrow}C_{k\uparrow} - C^{+}_{k+q\downarrow}C_{k+q\downarrow}) \tag{3.9}$$

3.2 The Greens Function Method

Green's functions have been very extensively used in the study of condensed matter states: superconductivity, magnetism and interplay of magnetism , internal energy, particle densities, magnetization, polarization, energy of the elementary excitations and excitations of condensed matter/solid state are determined by the corresponding Greens function. Response functions such as the electric and magnetic susceptibility, electric conductivity, transition probabilities and cross sections are directly related to the Greens function.

Historically the concept of GFs evolved from the work of Green in potential theory and contained the terms of a much wider formulation to solve problems.
One of the main advantages of the Greens functions method is the ability to calculate these observables in a certain approximation without knowledge of the wave functions [46].
Quantum field theory (QFT) is the theory of fields providing theoretical framework

widely used in particle physics and condensed matter physics, in formulating consistent quantum theories of many particle systems, especially in situations where particles may be created and destroyed. It is originated in the problem of computing the energy radiated by an atom when dropped from one quantum state to another of lower energy providing us with an efficient method of solving a given problem in terms of some approximation. The real many body problem begins with a system of particles that interact with one another where we can no longer consider the particles to act independently but must take into account the enormously complicated influence that each particle has on the behavior of all the others. Moreover, the theory utilizes the methods of second quantization where the inter particle interactions are represented in terms of particle creation and annihilation operators that the Hamiltonian describing the system requires [47].

In quantum field theory the Green's functions are the so called propagators. This name is based on the idea that, in order to find the important physical properties of a system, it is essential to know, not the detailed behavior of each particle in the system, but rather just the average behavior of one or two typical particles.

3.3 The double time temperature dependent Green's function

The method of the double time temperature dependent Green functions [48] in statistical mechanics are the appropriate generalizations of the correlation functions. They are useful in calculating the average of dynamical quantities, and they have great advantages when equations are framed and solved. The retarded and advanced Green functions $G_r(t,t')$ and $G_a(t,t')$ for the double time temperature dependent Green function $<< A(t); B(t') >>$ involving two Heisenberg operators A(t)

and B(t') is defined by

$$G_r(t,t') =<< A(t); B(t) >> r \tag{3.10}$$

$$G_r(t,t') = i\theta(t-t') < [A(t), B(t')] > r \tag{3.11}$$

and

$$G_a(t,t') =<< A(t); B(t') >> a \tag{3.12}$$

$$G_a(t,t') = i\theta(t-t') < [A(t), B(t')] > a \tag{3.13}$$

where $<< ... >> r, a$ are the abbreviated notations for the corresponding Green's function, the square brackets $[.., ..]$ denote a commutator or anticommutator, single pointed brackets $< ... >$ denote a thermal average over a canonical ensemble which is appropriate since the number of particles is not constant, and $\theta(t-t')$ is heaviside, a step function with the value unity when $t>t'$ and the value zero when $t<t'$ and can be shortly written as,

$$\theta(t,t') = 1, (t-t')>0$$

Or

$$\theta(t,t') = 0, (t-t')<0$$

3.4 Equation of Motion of the Green's Function

We now derive the equation of motion of the Green function. It is known that A(t) and B(t') satisfy equations of the form

$$i\frac{dA}{dt} = [A, H] \tag{3.14}$$

We now differentiate the Green's functions given by Eq. (3.18) and (3.20) where G denotes both G_r and G_a and obtain,

$$i\frac{dG}{dt} = i\frac{d}{dt} << A(t), B(t') >> \tag{3.15}$$

$$i\frac{dG}{dt} = i\frac{d}{dt}(\theta(t-t') < [A(t)B(t') - \eta B(t')A(t)] >) \tag{3.16}$$

$$i\frac{dG}{dt} = i\frac{d}{dt}\theta(t-t') < [A(t)B(t') - \eta B(t')A(t)] > + i\theta(t-t') < [i\frac{dA(t)}{dt}B(t') - \eta B(t')i\frac{dA(t)}{dt})] > \tag{3.17}$$

$$i\frac{dG}{dt} = \frac{d}{dt}\theta(t-t') < [A(t)B(t') - \eta B(t')A(t)] > + < [T\frac{dA(t)}{dt}, B(t')] > \tag{3.18}$$

$$i\frac{dG}{dt} = \frac{d}{dt}\theta(t-t') < [A(t), B(t')] > + << i\frac{dA(t)}{dt}, B(t') >> \tag{3.19}$$

Note that

$$\frac{d\theta(t-t')}{dt} = -\frac{d\theta(t-t')}{dt}$$

$$\theta(t-t') = \int_{\infty}^{t} \delta(t-t')dt$$

it can be verified that

$$\frac{d\theta(t-t')}{dt} = \delta(t-t') \tag{3.20}$$

Hence, using Eq. (3.21) and Eq. (3.26), Eq. (3.27) can be written as

$$i\frac{dG}{dt} = \delta(t-t') < [A(t); B(t')] > + << [A(t); H(t)]; B(t') >> \tag{3.21}$$

The Green function is given by

$$G(t-t') = \int_{-\infty}^{\infty} d\omega G(\omega) e^{-\omega(t-t')} \tag{3.22}$$

and delta function is also given by

$$\delta(t-t') = \frac{1}{2\pi}\int_{-\infty}^{\infty} d\omega e^{-\omega(t-t')} \tag{3.23}$$

Multiplying both sides of equation 3.28 by i

$$\omega\int_{-\infty}^{\infty} d\omega G(\omega) e^{-i\omega(t-t')} = \frac{1}{2\pi}\int_{-\infty}^{\infty} d\omega e^{-i\omega(t-t')} < [A(t); B(t')] >$$

$$+\theta(t-t') < [i\frac{dA(t)}{dt}; B(t')] > \tag{3.24}$$

The fourier transform of equation 3.31 can be obtained by Multiplying both sides by

$$\frac{1}{2\pi}\int_{-\infty}^{\infty} dt e^{i\omega'(t-t')}$$

Hence

$$\omega\int_{-\infty}^{\infty} d\omega G(\omega)\frac{1}{2\pi}\int_{-\infty}^{\infty} dt e^{i(\omega-\omega')(t-t')} =$$

$$\frac{1}{2\pi}\int_{-\infty}^{\infty} d\omega\frac{1}{2\pi}\int_{-\infty}^{\infty} dt e^{i(\omega-\omega')(t-t')}dt < [A(t); B(t')] >$$

$$+ F.Tof\theta(t-t') < [i\frac{dA}{dt}; B(t')] > \tag{3.25}$$

which can be rewritten as

$$\omega\int_{-\infty}^{\infty} G(\omega)\delta(\omega-\omega')d\omega =$$

$$\frac{1}{2\pi}\int_{-\infty}^{\infty} G(\omega)\delta(\omega-\omega')d\omega < [A(t); B(t')] > + << [A; H]; B >> \tag{3.26}$$

and in its simplified form

$$\omega G(\omega) = \frac{1}{2\pi} < [A; B] > + << [A; H]; B >> \tag{3.27}$$

where

$$\frac{1}{2\pi}\int_{-\infty}^{\infty} e^{i(\omega-\omega')(t-t')}dt = \delta(\omega-\omega')$$

and

$$\delta(\omega-\omega') = 1, \omega = \omega'$$

Hence

$$\omega G(\omega) = \frac{1}{2\pi} < [A; B] > + << [A; H]; B >> \tag{3.28}$$

The only other equation which we shall require from Green function theory is that defining the relationship between $<< A; B >>_{\omega}$, if it is denoting the Fourier transform of the Green function involving operators A(t) and B(t) and it's related correlation function $< B(t)A(t) >$. This may be written as

$$< B(t')A(t) >= \lim_{\varepsilon \to 0^+} \int_{-\infty}^{\infty} \frac{<< A; B >>_{\omega+i\varepsilon} - << A; B >>_{\omega-i\varepsilon} e^{i\omega(t-t')} d\omega}{e^{\frac{\hbar\omega}{K_B T}} - 1} \tag{3.29}$$

we can rewrite equation 3.28 in terms of boson creation and annihilation operators as

$$\omega << a_{k\uparrow}; a^+_{k\uparrow} >>= \frac{1}{2\pi} < [a_{k\uparrow}; a^+_{k\uparrow}] > + << [a_{k\uparrow}; H]; a^+_{k\uparrow} >>_{\omega} \tag{3.30}$$

Substituting total Hamiltonian written in equation 3.9 into the simplified form of Green function written in equation 3.30 the resulting expression becomes,

$$\begin{aligned} \omega << a_{k\uparrow}; a^+_{k\uparrow} >>= \frac{1}{2\pi} + (Js(ka)^2 - 2Ds - g\mu_B H - \mu E) << a_{k\uparrow}; a^+_{k\uparrow} >> \\ - \frac{\lambda}{N}(<< a_{k\uparrow} C^+_{k\uparrow} C_{k\uparrow}; a^+_{k\uparrow} >> - << a_{k\uparrow} C^+_{k+q\downarrow} C_{k+q\downarrow}; a^+_{k\uparrow} >>) \end{aligned} \tag{3.31}$$

Employing the following decoupling procedure on the higher order Green's function,

$$\begin{aligned} << a_{k\uparrow} C^+_{k\uparrow} C_{k\uparrow}; a^+_{k\uparrow} >>=<< [a_{k\uparrow} C^+_{k\uparrow} C_{k\uparrow}; H]; a^+_{k\uparrow} >> \\ \simeq < C^+_{k\uparrow} C_{k\uparrow} >< a_{k\uparrow}; a^+_{k\uparrow} >> \end{aligned} \tag{3.32}$$

Using similar procedure

$$\begin{aligned} << a_{k\uparrow} C^+_{k+q\downarrow} C_{k+q\downarrow}; a^+_{k\uparrow} >>=<< [a_{k\uparrow} C^+_{k+q\downarrow} C_{k+q\downarrow}; H]; a^+_{k\uparrow} >> \\ \simeq < C^+_{k+q\downarrow} C_{k+q\downarrow} >< a_{k\uparrow}; a^+_{k\uparrow} >> \end{aligned} \tag{3.33}$$

Inserting equation(3.32-3.33) into equation(3.31) we obtain

$$\omega << a_{k\uparrow}; a^+_{k\uparrow} >>= \frac{1}{2\pi} + (Js(ka)^2 - 2DS + g\mu_B H + \mu E) << a_{k\uparrow}; a^+_{k\uparrow} >> + m\lambda << a_{k\uparrow}; a^+_{k\uparrow} >> \tag{3.34}$$

where

$$m = \frac{1}{N}\sum_{k,q}(< C^{+}_{k\uparrow}C_{k\uparrow} > - < C^{+}_{k+q\downarrow}C_{k+q\downarrow} >)$$

Is the carrier spin polarization.

λ is an interaction coupling constant, and assuming that

$$\beta' = JSa^2$$

Then

$$\omega << a_{k\uparrow}; a^{+}_{k\uparrow} >>= \frac{1}{2\pi} + (\beta' k^2 - 2DS + g\mu_B H + \mu E) << a_{k\uparrow}; a^{+}_{k\uparrow} >> + m\lambda << a_{k\uparrow}; a^{+}_{k\uparrow} >> \tag{3.35}$$

Equation(3.35) can be rewritten as

$$(\omega - \beta' k^2 + 2Ds - g\mu_B H - \mu E - m\lambda) << a_{k\uparrow}; a^{+}_{k\uparrow} >>= \frac{1}{2\pi} \tag{3.36}$$

Hence

$$<< a_{k\uparrow}; a^{+}_{k\uparrow} >>= \frac{1}{2\pi}\frac{1}{\omega - \beta' k^2 + 2Ds - g\mu_B H - \mu E - m\lambda} \tag{3.37}$$

$$G(\omega)_k = \frac{1}{2\pi}(\frac{1}{\omega - \beta' k^2 + 2Ds - g\mu_B H - \mu E - m\lambda}) \tag{3.38}$$

Get the GF find to obtain disperssion relation, from the poles of Green's function we can obtain the excitation spectrum of magnon as

$$\omega_k = \beta' k^2 - 2Ds + g\mu_B H + \mu E - m\lambda \tag{3.39}$$

where

$$\gamma = -2Ds + g\mu_B H + \mu E + m\lambda$$

$$\omega_k = \beta' k^2 + \gamma \tag{3.40}$$

The dispersion equation (equation 3.40) describes the spin wave energy as a function of wave vector k. This spin wave energy depends on external elecric field, magnetic field, and their coupling term(mutual interaction of two fields).

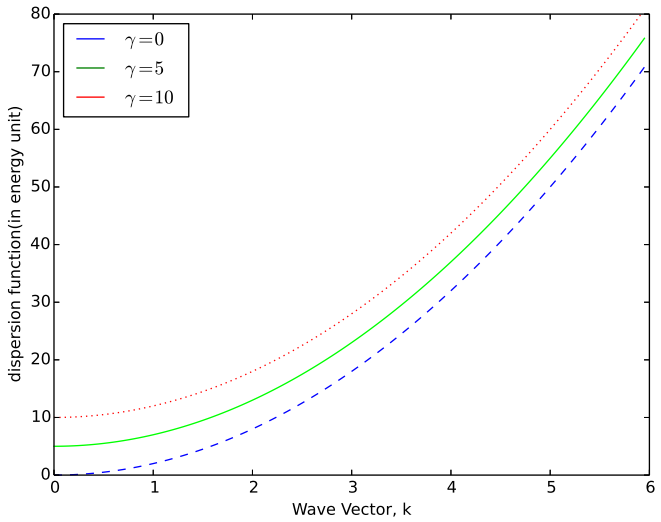

Fig. 3.1: Calculated spin wave density subjected to various EEF.

In figure 3.1 a significant change in the dispersion relation is observed at different γ values. This can be used to modify the property of the multiferroics up on appropriate selection of the electric field, where we have seen that spin wave energy is increasing with the increasing of EEF. This is to mean that the magnetic moments of system are aligned ordely in the direction of applied fields. Dispersion develops energy gap when subjected to various fields.

3.5 Properties of multiferroics

3.5.1 Magnetization

Before studying the magnetization of system first we have to compute the number of magnons excited at temperature T using the Correlation function as

$$< a_{k\uparrow}(t')^{+}; a_{k\uparrow}(t) >= lim_{\epsilon\to 0} \int_{-\infty}^{\infty} \frac{e^{-i\omega(t-t')}}{e^{\beta\omega}-1}(G(\omega+\epsilon)_k - G(\omega-\epsilon)_k) \tag{3.41}$$

The equal time(t=t') correlation gives the number of magnons and is obtained as

$$< n_k >= \frac{1}{e^{\beta\omega}-1} \tag{3.42}$$

Magnetization is the order parameter to study ferromagnetism or Antiferromagnetism in multiferroic materials, and given by

$$M(T) = M(0) - m(T) \tag{3.43}$$

Where

$$M(0) = g\mu_B NS \tag{3.44}$$

And

$$m(T) = g\mu_B \sum_k \frac{1}{e^{\beta\omega_k} - 1} \tag{3.45}$$

Changing summation in to integration and consider 2D coordinate system magnetization can be rewrite

$$m(T) = \frac{g\mu_B}{2\pi^2} \int_0^\infty \frac{kdk}{e^{\beta\omega_k} - 1} \tag{3.46}$$

Let

$$x = \omega_k = \beta' k^2 + \gamma$$

Then

$$\frac{dx}{2\beta'} = kdk$$

And we consider low temperature case, and taking the following approximations

$$e^{\beta\omega_k} - 1 \approx e^{\beta\omega_k}$$

Using these equation(3.46) takes the following form

$$m(T) = \frac{g\mu_B}{(2\pi)^2} \int_\gamma^\infty e^{-x/K_B T} dx \tag{3.47}$$

After integration we get

$$m(T) = \frac{g\mu_B}{\beta'(2\pi)^2} K_B T e^{\frac{-\gamma}{K_B T}} \tag{3.48}$$

Substituting equation(3.44) and equation(3.47) into equation(3.43) we obtained the total magnetization.

$$M(T) = g\mu_B NS - \frac{NSg\mu_B}{\beta'(2\pi)^2 NS} K_B T e^{\frac{-\gamma}{K_B T}} \tag{3.49}$$

$$M(T) = M(0) - \frac{NSg\mu_B}{NS\beta'(2\pi)^2} K_B T e^{\frac{-\gamma}{K_B T}} \tag{3.50}$$

Assume that $A = \frac{K_B}{(NS)^2\beta'(2\pi)^2}$ then we obtain,

$$\frac{M(T)}{M(0)} = 1 - ATe^{\frac{-\gamma}{K_B T}} \tag{3.51}$$

From this equation it is clear that reduced magnetization is varied with temperature. Equation 3.51 describes reduced magnetization is highly affected by the external electric and magnetic fields and their coupling term.

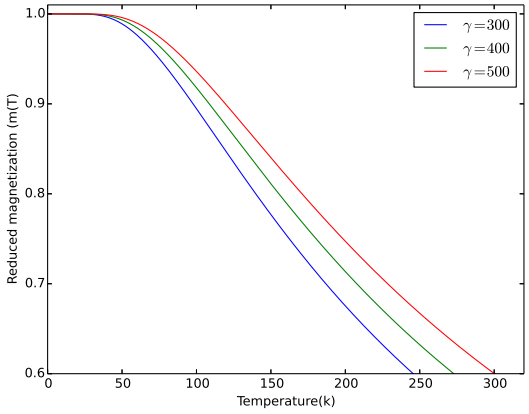

Fig. 3.2: Calculated reduced magnetization as a function of temperature subjected to various fields.

From figure 3.2 magnetization of the system tends to increase towards the transition temperature as the electric field parameter increase. This external electric field can change crystal shape, lattice structure and density of states system. The impact of the external fields on the magnetization is in agreement with the experimental work [49–52].

The total magnetization dependence on the external electric field subjected to various magnetic field is shown in figure 3.3. It is clear that magnetization of the

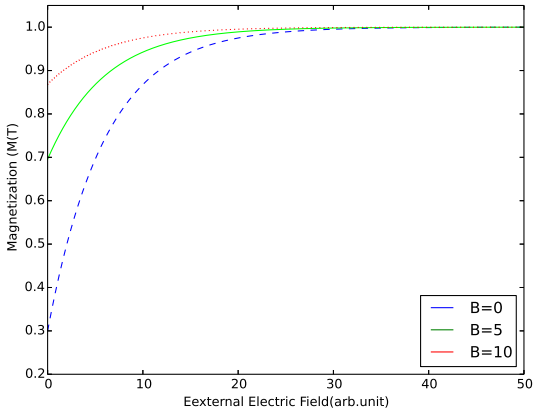

Fig. 3.3: Calculated magnetization as a function of EEF subjected to various magnetic fields.

system increases as external two fields increase, resulting in the enhancement of the critical temperature T_c.

3.5.2 Magnetic Susceptibility

Is one measure of the magnetic properties of a material. The susceptibility indicates whether a material is attracted into or repelled out of a magnetic field, which in turn has implications for practical applications. Quantitative measures of the magnetic susceptibility also provide insights into the structure of materials, providing insight into bonding and energy levels. It is symbolized by χ_m.

If χ_m is positive, a material can be paramagnetic. In this case, the magnetic field in the material is strengthened by the induced magnetization. Alternatively, if χ_m is negative, the material is diamagnetic. In this case, the magnetic field in the material is weakened by the induced magnetization. Generally, non magnetic materials are said to be para or diamagnetic because they do not possess permanent magneti-

zation without external magnetic field. Ferromagnetic, ferrimagnetic, or antiferromagnetic materials have positive susceptibility and possess permanent magnetization even without external magnetic field.

Magnenetic susceptibility χ_m is given by

$$\chi_m = \frac{\partial M(T)}{\partial H}|_H \longrightarrow 0 \tag{3.52}$$

Where $M(T)$ is

$$M(T) = g\mu_B NS - \frac{NSg\mu_B}{\beta'(2\pi)^2 NS} K_B T e^{\frac{-\gamma}{K_B T}}$$

After doing certain mathematical manipulation we obtained the following equation

$$\chi_m = \frac{(g\mu_B)^2}{\beta'(2\pi)^2} e^{\frac{-(-2Ds+\mu E)}{K_B T}} \tag{3.53}$$

we can represent

$$\sigma = -2Ds + \mu E$$

Implies that

$$\chi_m = \frac{(g\mu_B)^2}{NS\beta'(2\pi)^2} e^{\frac{-\sigma}{K_B T}} \tag{3.54}$$

From equation 3.53 magnetic susceptibiity is highly affected by the applied external electric field.

Figure 3.4 demonstrates effect of EEF on magnetic susceptibility.From this figure we have seen that control of magnetic susceptibility of multiferroic material by an external electric field.

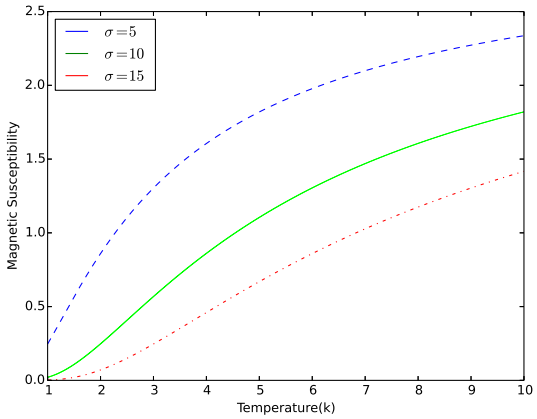

Fig. 3.4: Magnetic susceptibility as a function of temperature subjected to various EEF.

3.5.3 Specific heat capacity

To obatin the specific heat capacity, first we have to find an expression for internal energy of system.

$$U = \sum_k n_k \omega_k \tag{3.55}$$

Then the mean number of spin waves with wave vector k at temperature T is given by:

$$< n_k >= \frac{1}{e^{\beta\omega} - 1} \tag{3.56}$$

$$\omega_k = \beta' k^2 - 2Ds + g\mu_B H + \mu E + m\lambda$$

Is dispresion relation of multiferroics.

Substituting this relation in equation (3.65), gives:

$$U = \sum_k (\beta' k^2 + \gamma) \frac{1}{e^{\beta\omega} - 1} \tag{3.57}$$

$$U = \frac{1}{(2\pi)^2} \int_0^\infty (\beta' k^2 + \gamma) \frac{1}{e^{\frac{\beta' k^2 + \gamma}{k_B T}} - 1} k dk \tag{3.58}$$

For low temperature, assuming that

$$\frac{1}{e^{\frac{\beta' k^2+\gamma}{k_B T}}-1} \approxeq e^{-\frac{\beta' k^2+\gamma}{k_B T}}$$

Let

$$x = \beta' k^2 + \gamma$$

Then

$$kdk = \frac{dx}{2\beta'}$$

Hence we can rewrite

$$U = \frac{1}{2\beta'(2\pi)^2} \int_{\gamma}^{\infty} \frac{xdx}{e^x/k_\beta T} \tag{3.59}$$

We find the total energy of multiferroic system for 2D coordinate system

$$U \approxeq \frac{1}{\beta'(2\pi)^2}(k_B T + \gamma) k_B T e^{-\frac{\gamma}{k_B T}} \tag{3.60}$$

from this figure it is clear that internal energy of system depends on field compo-

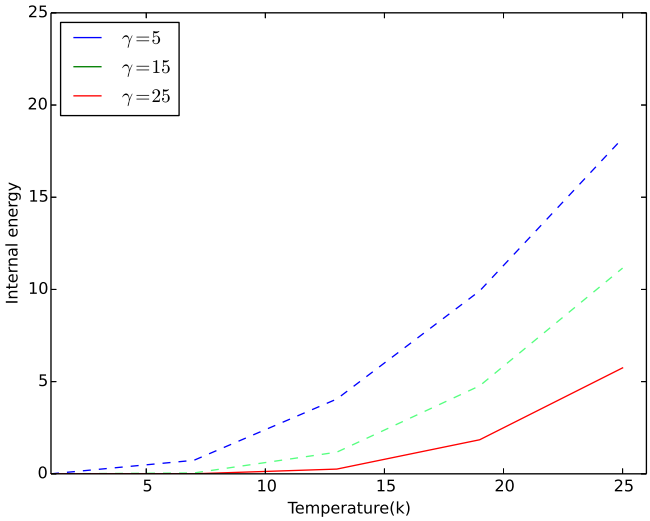

Fig. 3.5: Internal energy as a function of temperature subjected to various EEF.

nents, coupling term and temperature.

Specific heat capacity does not depend on an objects mass, it depends on the type of material. It is defined as the amount of heat that a unit mass of a material must gain or lose to change its temperature by a given amount.

$$C = \frac{\partial U(T)}{\partial T} \tag{3.61}$$

Up on Substituting equation 3.59 into equation 3.60 and doing derivatives energy with respect to temperature, we find expression for specific heat capacity of system under study.

$$C = \frac{K_B}{\beta'(2\pi)^2}[2K_BT + \frac{\gamma^2}{K_BT} + \gamma]e^{-}\frac{\gamma}{k_BT} \tag{3.62}$$

From this equation we can study the actual situation occurring in the temperature and fields dependent behavior of specific heat capacity in multiferroic materials. Figure 3.6 represents variation of specific heat capacity with temperature

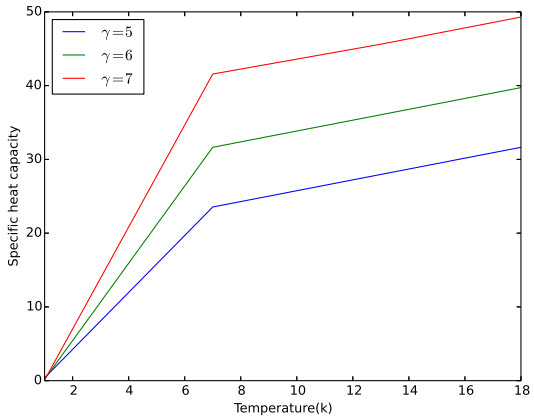

Fig. 3.6: specific heat capacity as a function of temperature subjected to various EEF.

subjected to various EEF. As the field increases the specific heat also increases until it reaches a saturation region.

4

Computational Material Science

4.1 Introduction

The advanced and accurate knowledge of materials especially at atomic and molecular levels are essential for performing various desired technological functions bringing about revolution in modren day life. Progress in computational matrials science with the development of variety of computational methodologies has opened up a number of new horizons regarding exploration of material properties having at most technological importance.

A wide range of material properties can be predicted with great precision before executing the experimental investigation, which could avoid expensive, tedious and time consuming exercise. While predicting a certain phenomenon,designing a novel material or investigating its characterstic properties at atomic level computational material science has been proved to be significant importance.The trend in designing functional materials with reduced(nanometer) size consisting of few hundreds of atoms only and to improve the accuracy, it has become inevitable to go beyond the previously used Newtonian mechanics, which lacks accuracy and unable to deal with small systems down to nanometers scale.

Thanks to the development of efficient techniques like first principles calculations and the availablity of increased computer simulation power. The density func-

tional theory based first principles calculations has been found promising while investigating the novel functional nanostructures.

4.1.1 Density Functional Theory (DFT)

Is a computational quantum mechanical modelling method used in physics, chemistry and materials science to investigate the electronic structure (principally the ground state) of many-body systems, in particular atoms, molecules, and the condensed phases. Using density functional theory, the properties of a many electron system can be determined by using functionals, i.e. functions of another function, which in this case is the spatially dependent electron density. Hence the name density functional theory comes from the use of functionals of the electron density.

DFT is among the most popular and versatile methods available in condensed matter physics, computational physics, and computational chemistry. DFT has been very popular for calculations in solid state physics since the 1970s. ,However, DFT was not considered accurate enough for calculations in quantum chemistry until the 1990s, when the approximations used in the theory were greatly refined to better model the exchange and correlation interactions.

Computational costs are relatively low when compared to traditional methods, such as exchange only Hartree Fock theory and its descendants that include electron correlation. DFT is Working with electron density rather than wave function(describes the quantum state of a particle in an isolated system). DFT Reduces 3N dimensions of system into exactly 3 dimensions.

4.1.2 Many body problem

In order to study the materials properties in solid state physics, which generally have large number of atoms ($\sim 10^{23}$) the solution of many body problems become

inevitable. While studying such systems, where large number of atoms(many electrons and nuclei) interacts with each other, their properties can be determined by solving the schrodinger equation.

$$H\psi(r,R) = E\psi(r,R) \tag{4.1}$$

The hamiltonian is

$$H = -\sum_{i}\frac{\hbar^2\nabla_i^2}{2m_e} - \sum_{I}\frac{\hbar^2\nabla_i^2}{2M_I} + \frac{1}{2}\sum_{i\neq j}\frac{e^2}{r_i - r_j} + \frac{1}{2}\sum_{i\neq j}\frac{Z_I Z_J e^2}{R_i - R_j} - \sum_{i,I}\frac{Z_I e^2}{r_i - R_I} \tag{4.2}$$

Here in equation 4.2 the term $\hbar = \frac{h}{2\pi}$ represents reduced palnck's constant, m_e, r_i and e are the mass, position,and charge of the electron i^{ith} respectively. Where M_I, R_I and Z_I represents the mass, position ,and charge of the I^{ith} nuclei respectively. The first two terms give the kinetic energies of electron and nuclei where as the remaining terms represents the electron electron ,nuclei nuclei and electron nuclei interactions respectively.

For any other system consisting of large number of electrons and nuclei, it is inevitable to employ some approximations, even for helium. One of the most extensively used approximation method in almost all the methodologies is Born Oppenheimer approximation [53].

Under this approximation we can consider the wave functions of both electron and nuclei separately. As the motion of electron is much higher than that of nuclei due to its larger mass, so the nuclei can be considered as stationary. Hence the kinetic energy of nuclei can be neglected due to its frozen equilibruim state. This leads to the fact that the nuclei can be treated as external potential V_{ext} applied to the fast moving electrons. By considering the wave functions of electron $\psi_{e(r.R)}$ and the nuclei $\psi_{N(r.R)}$ separately we will have

$$H\psi(r,R) = \psi_{e(r.R)}\psi_{N(r.R)} \tag{4.3}$$

And the schrodinger equation for only electrons will take the form

$$H_e\psi_{e(r.R)} = E_e\psi_{e(r.R)} \tag{4.4}$$

After applications of Born Oppenheimer application, the Hamiltonian will be

$$H = -\sum_i \frac{\hbar^2\nabla_i^2}{2m_e} + \frac{1}{2}\sum_{i\neq j}\frac{e^2}{r_i - r_j} - \sum_{i,I}\frac{Z_I e^2}{r_i - R_I} \tag{4.5}$$

Though treatment of the systems look much simplified now, but still in case of large number of electrons, computational cost would be very high and unaffordable. The electron-electron interaction represented by the third term of equation 4.5 needs further application, as it cannot be tackeled with this application only. In order to deal with this problem other approximation like Density functional theory(DFT) has been employed, which will be described in the following briefly.

4.1.3 The Hohenberg Kohn theorems

First Hohenberg Kohn theorem: The ground state density n(r) of a many body quantum system in some external potential v(r) uniquely determines the potential. Hence according to DFT, all properties of a many body system can be determined by the ground state charge density.

$$\Psi(r_1, ...r_n) = n(r) = \sum_i \varphi_i^2 \tag{4.6}$$

Hohenberg Kohn theorem

The ground state energy(the most stable state of the system) is also uniquely determined by the ground state charge density: the density that minimizes the total energy is the exact ground state density.

$$E[n(r)] = \langle T + U + V\rangle = \langle T + U\rangle + \langle V\rangle = F[n(r)] + n(r)v(r)dr \tag{4.7}$$

Where $H = T + U + V$, is the many electron Hamiltonian, Ψ is ground state wave function, T is the kinetic energy, U is the electron electron interaction, V is

the external potential, and $n(r)$ is the charge density. The universal functional F of the density is $F[n(r)] = \langle T + U \rangle$. The Functional includes the kinetic energy of the electrons $T_s[n]$, Hartree classical Coulomb repulsion energy $E_H[n]$, and the exchange and correlation energies $E_{xc}[n]$.

$$F[n(r)] = T_s[n] + E_H[n] + E_{xc}[n] \tag{4.8}$$

4.1.4 Kohn Sham equation

In 1965, Kohn and Sham showed that it is possible to reduce the many body quantum mechanical problem to an exactly equivalent set of one electron equations, solved self consistently. This is a reformulation of the following idea. The system of interacting electrons is mapped on to an auxiliary system of non interacting electrons having the same ground state charge density $n(r)$. In Kohn Sham equation the Schrodingers equation for the system takes the following form:

$$[\frac{\hbar^2 \nabla_i^2}{2m} + V(r)_{ion} + V(r)_H + V_{XC}[n(r)]]\varphi_i(r) = \varepsilon_i \varphi_i(r) \tag{4.9}$$

The first term is the energy of non interacting electrons. The second term $V(r)_{ion}$ is the ionic potential describing the attractive interaction between electrons and nuclei. The third term (called the Hartree potential) contains the electrostatic interactions between clouds of charge.

$$V(r)_H = \int \frac{n(r')e^2 d^3r}{|r_i - r_j|} \tag{4.10}$$

The fourth term is called the exchange and correlation potential.

$$V_{XC}[n(r)] = \frac{\delta E_{xc}}{\delta n(r)} \tag{4.11}$$

The nature of this external potential defines the physical properties of the system and thus is extremely important. Ground state electronic energies ε_i and wave functions $\varphi i = |i, k >$ can be obtained as the result of the DFT calculation. In many

cases very good agreement with experiment is achieved when the exchange and correlation potential is treated using the rather simple local density approximation (LDA) [54–57]. A large variety of important scientific results have been and are still being obtained using LDA and the generalized gradient approximations (GGA)

4.2 Exchange correlation functionals

The only unknown term in Eq.(4.9) is the exchange correlation functional term, which needs to be approximated in order to use Khon sham equation for practical purposes. Two extensively used approximations for this purpose are local density approximation(LDA) and the generalized gradient approximation(GGA).

4.2.1 Local Density Approximation

The two main types of exchange/correlation functionals used in DFT are the local density approximation(LDA) and the generalized gradient approximation(GGA).

In the LDA, the exchange correlation functional is defined for an electron in a uniform electron gas of density n. [78] It is exact for a uniform electron gas, and is anticipated to be a reasonable approximation for slowly varying densities. In molecules and solids, however, the density tends to vary substantially in space. Despite this, the LDA has been very successfully used in many systems. It tends to predict overbonding in both molecular and solid systems, [79] and it tends to make semiconductor systems too metallic (the band gap problem). [80]

$$E_{xc}^{LDA}[n] = \int \varepsilon_{xc}^{hom}(n(r))n(r)dr \tag{4.12}$$

The exact exchange correlation energy for the homogeneous electron gas was computed by Cperley and Alder using the Quantum Monte Carlo method, which was then parameterized in a functional form by Perdew and Zunger. The Local Density

approximation can further be extended to an other approximation called Local Spin Density Approximation (SDA) for the treatments of magnetic materials. In this case the spin dependence of the correlation energy density is computed by introducing the relative spin-polarization. LDA is powerful in describing many properties of systems. But it has also a limitation based on the assumption that the electron density around an atom to be homogeneous.

4.2.2 Generalized Gradient Approximation(GGA)

This approach includes more physical information than LDA. The generalized gradient approximation includes corrections for gradients in the electron density, and is often implemented as a corrective function of the LDA. The form of this corrective function, or "exchange enhancement" function determines which functional it is, e.g. PBE, RPBE, revPBE, etc [81].

GGA can be expressed as

$$E_{xc}^{GGA}[n] = \int \varepsilon_{xc}^{GGA}(n(r), |\nabla n(r)|)n(r)dr \tag{4.13}$$

There are two commonly used functionals in calculations involving solids. These are the Perdew Wang functional (PW91) and the Perdew Burke Ernzerhof functional (PBE). In summary, in order to better describe correlation effects in some strongly correlated systems such as compounds with transition metals (3d electrons) and lanthanide (4f electrons), several extensions to LDA and GGA have been made. Such as Coulomb parameter U and Hunds exchange parameter J are included for the d and f electrons, LDA+U, etc. plane wave basis set and Pseudopotentials A plane wave basis set is defined as

$$< r|k+G >= \frac{1}{\sqrt{V}} e^{i(k+G).r} \tag{4.14}$$

$$\frac{\hbar^2 \nabla_i^2}{2m} \frac{|k+G|}{2} < Ecut, \tag{4.15}$$

where G is the reciprocal vector, V is the crystal volume, E_{cut} is a cutoff on the kinetic energy of PWs. PWs are simple to use and the basis is fixed by the crystal structure and by the cutoff. It allows to check the convergence by changing the cutoff. The pseudopotential method is based on the fact that the va lence electrons are responsible for most chemical and physical properties of molecules and solids. There are different Pseudopotentials, including norm conserving and ultrasoft.

4.3 Force Theorem

The force acting on an ion while performing DFT calculations are supposed to be zero or should reach a specified criteria in order to attain the exact ground state configuration. The term geometry optimization refers to the configuration where the position of the ions as well as the shape and volume of the cell is also converged. The Hellman Fynman theorem can be used to calculate the Force F acting on at a position R by

$$F = -\frac{\partial E}{\partial R} \tag{4.16}$$

The total energy of the system can be expressed as

$$E = \frac{<\Psi|H|\Psi>}{<\Psi|\Psi>} \tag{4.17}$$

In Eq.(4.17) Ψ represents the wave function and it needs to be normalized, so Eq.(4.16) will take the form

$$F = -<\Psi|\frac{\partial H}{\partial R}|\Psi> - <\frac{\partial \Psi}{\partial R}|H|\Psi> - <\Psi|H|\frac{\partial \Psi}{\partial R}> \tag{4.18}$$

In the case of ground state energy the wave function will have

$$F = -<\Psi|\frac{\partial H}{\partial R}|\Psi> \tag{4.19}$$

4.4 Self consistent algorithm

Figure 4.1 shows schematically illustrates the major steps of a density functional self consistent loop. It is known that density functional theory is a self consistent field (SCF) method. This means that the calculation runs in cycles, and convergence is achieved when the results given by solving the SCF equations are consistent with the assumptions made at the beginning of the cycle. In DFT the main quantity that is calculated and checked for self consistency, is the electronic density.

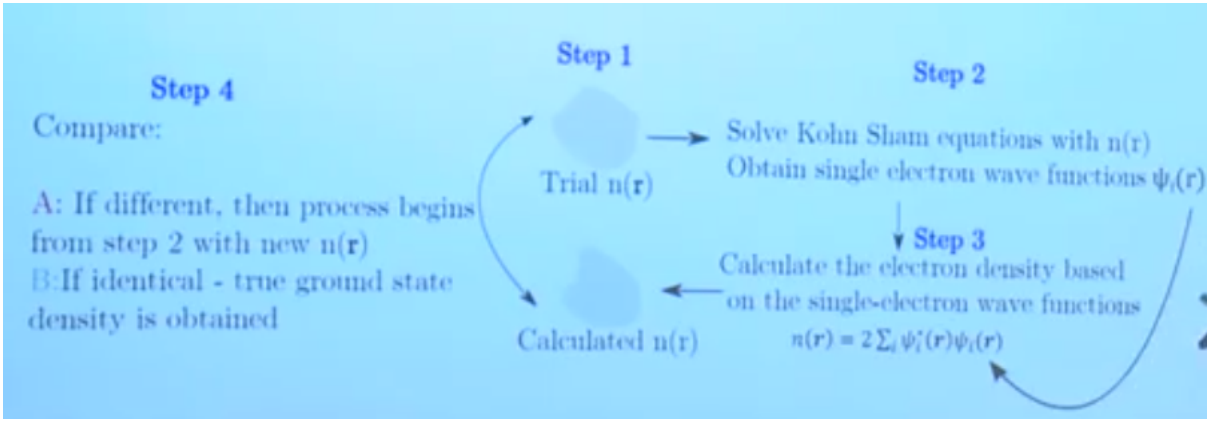

Fig. 4.1: Schematic representation of the self consistent algorithm for a density functional based calculation [58].

4.5 Effect of pressure on Density of states for $BiFeO_3$

The density of states refers to the number of electronic states in a particular energy range. In this section we are going to study the density of states of $BiFeO_3$ in relation to pressure which is varied by changing the universal scaling lattice parameter in Poscar input file. we have reduced the experimental scaling lattice parameter from 1Å in to 0.99Å, 0.98Å, 0.97Å 0.96Å,0.95Å, 0.94Å, 0.93Å and 0.92Å to find out the effect of pressure on the density of state of the system under study.

In order to have a profound understanding about the origin and the character-

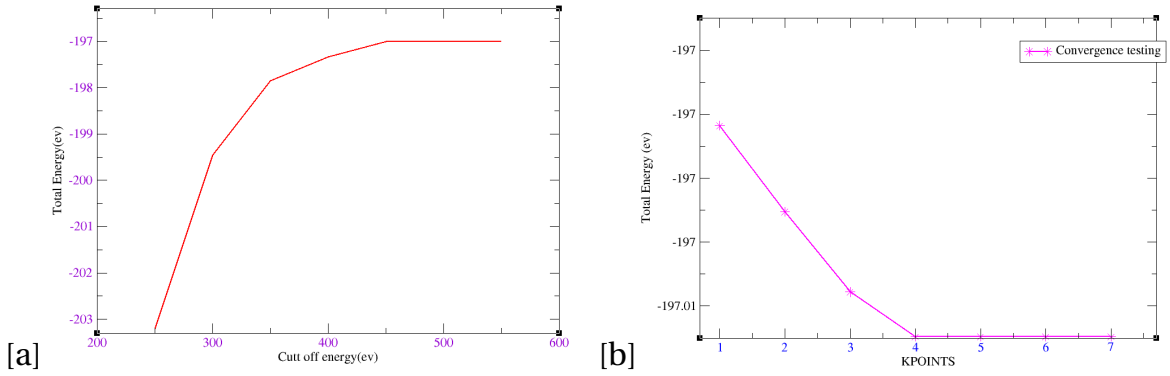

Fig. 4.2: Figure a) represents dependence of the total energy on ENCUT and b) represents k-point convergence of the total energy of BiFeO_3 molecule.

istics of multiferroic material($BiFeO_3$), we have conducted a systematic theoretical study based on the first principles electronic structure calculations of this material under external hydrostatic pressure. Our results suggest density of state (DOS) at the Fermi level decreasing with increasing the pressure.

The structural and electronic properties have been investigated based on density functional theory (DFT), as implemented in the VASP package. The Generalized Gradient Approximation (GGA) is a type of exchange correlational functional that has been employed in this work.

From figure 4.2, we can see that it takes a cutoff energy of about 500eV to achieve a convergence level around -197eV. The reason we do not just use very high ENCUT all the time is it is very expensive. Based on this figure, we need at least a 6 x 6 x 2 kpoint grid to achieve a convergence. Sometimes very dense grids (e.g. up to 9 x 9 x 3) are needed for highly converged properties such as the density of states in smaller unit cells. Oscillations in the total energy are typical, and it can be difficult to get high levels of convergence. The best practices are to use the same kpoint sampling grid in energy differences where possible, and dense (high numbers of kpoints) otherwise. As unit cells get larger, the number of kpoints required becomes

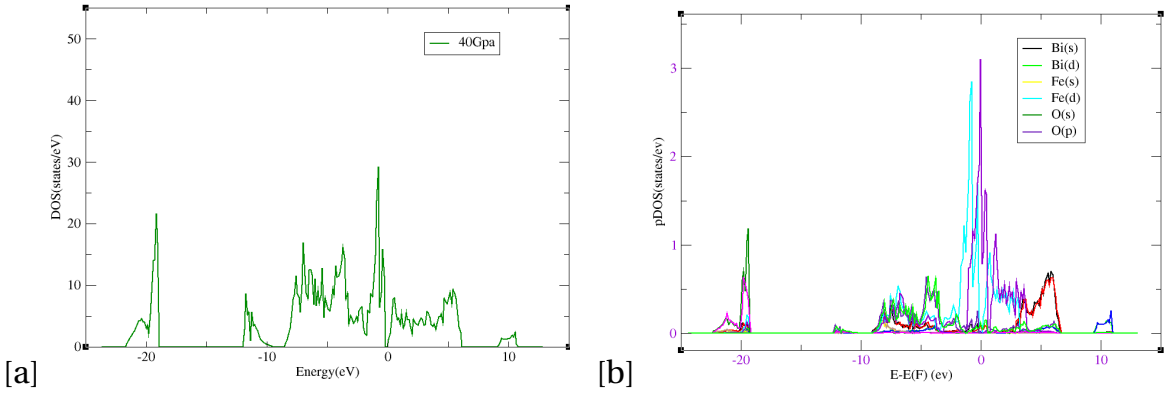

[a] [b]

Fig. 4.3: Total(a) and partial(b) density of states at 40Gpa pressure respectively.

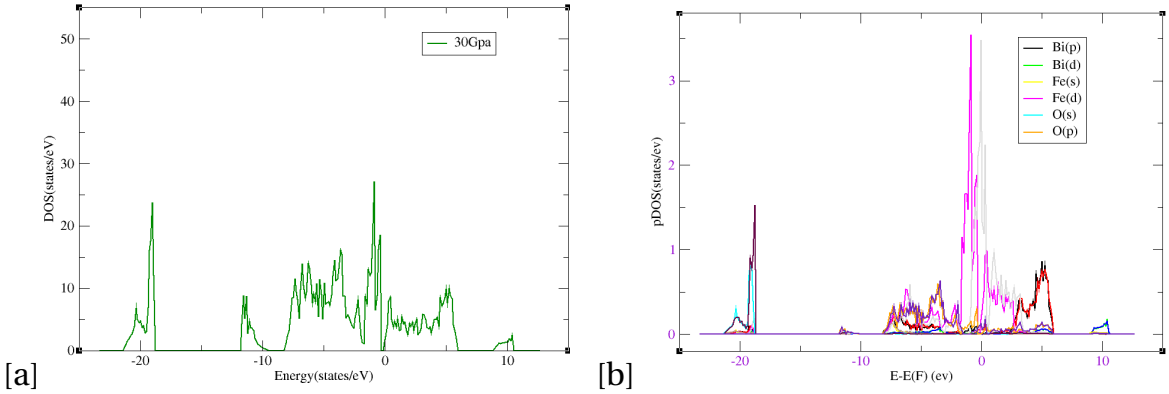

[a] [b]

Fig. 4.4: Total(a) and partial(b) density of states at 25Gpa pressure respectively.

smaller. In other words, doubling the unit cell vectors results in a halving of the number of kpoints.

As pressure increases the lattice parameter decreases exponentially. The electronic structure of BiFeO_3 shows that the top of valance band which means near to fermi energy is occupied by O(s), O(p), Bi(p), and Bi(d) states, The bottom of conduction band is occupied dominantly by Bi(p) Bi(d) and Fe(d) states.

The evolution of density of states (PHDOS) with increasing hydrostatic pressure for BiFeO_3 is demonstrated. This findig is in reasonable agreement with already reported theoretical work.

It is observed that if one goes on increasing the pressure, it has been found that above 5GPa, the DOS decreases significantly near the vicinity of the Fermi level.

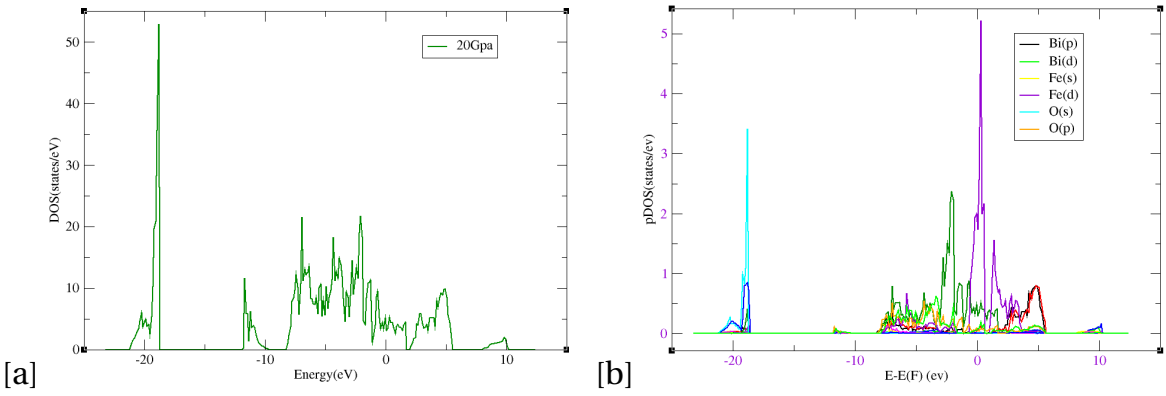

[a] [b]

Fig. 4.5: Total(a) and partial(b) density of states at 20Gpa pressure respectively.

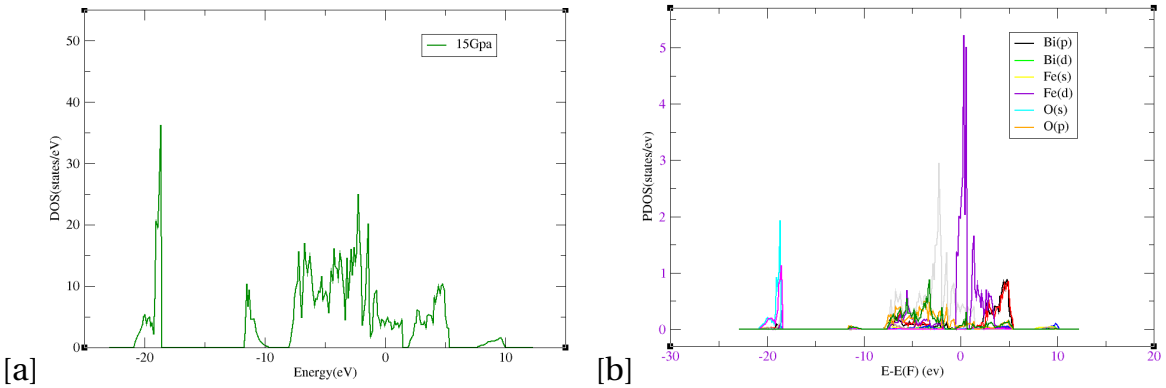

[a] [b]

Fig. 4.6: Total(a) and partial(b) density of states at 15Gpa pressure respectively.

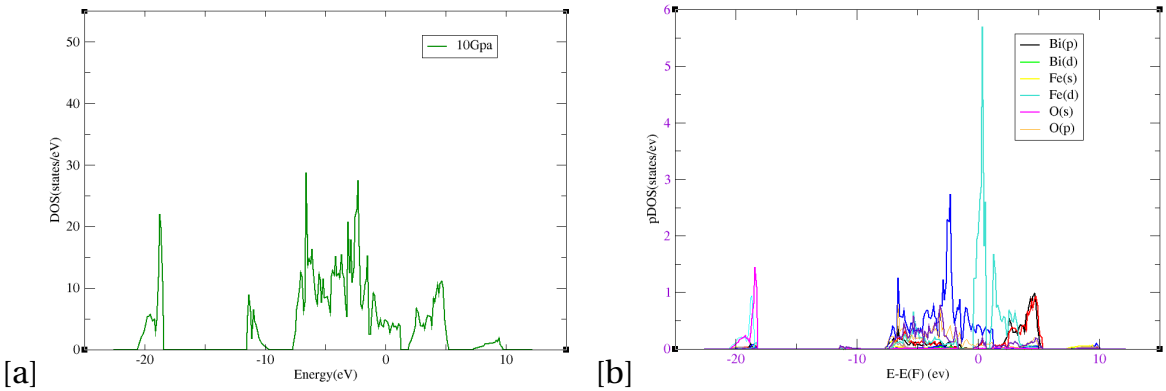

[a] [b]

Fig. 4.7: Total(a) and partial(b) density of states at 10Gpa pressure respectively.

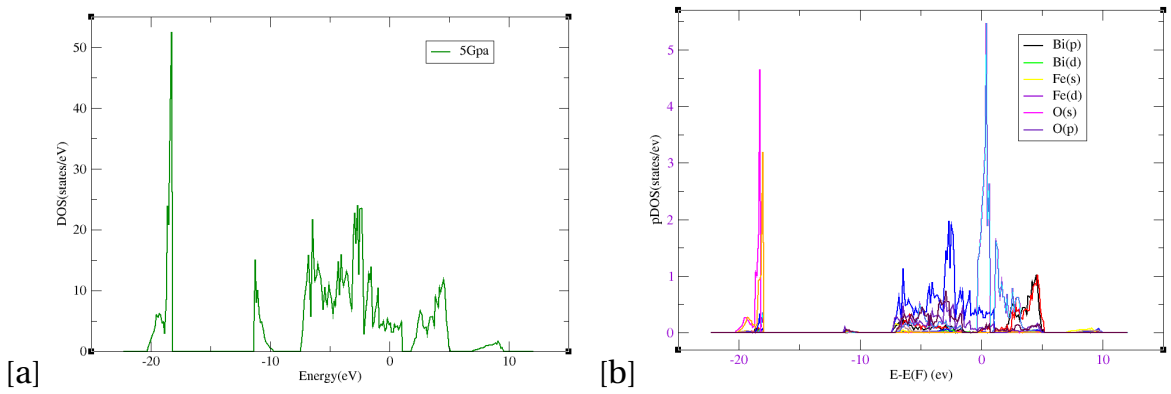

Fig. 4.8: Total(a) and partial(b) density of states at 5Gpa pressure respectively.

The bottom of conduction band is occupied dominantly by Fe(d) and Bi(p) states. The conduction band is dominatly occupied by Bi(d) state.

4.6 Optical properties of $BiFeO_3$

In principle optical properties can be probed by using shining light(photon) into the sample that results in the electronics excitations. The adsorption of photon is related to the two type of electronic excitations namely inter band and intra band transition. The former accounts for the transition of excited electrons from the valance to the conduction band to create holes in the valance band, while the latter is the transition between the distinct energy levels with in the the valance band or conduction band. The photon adsorption can be obtained from the imaginary part of the dielectric function. In this, we determine the imaginary part of macroscopic dielectrics functions in the long wave length limit($q \longrightarrow = 0$) according to the expression

$$\varepsilon^{(2)}_{\alpha\beta}(\omega) = \frac{4\pi^2 e^2}{\Omega} lim \frac{1}{q^2} \sum_{c,v,k} 2\omega_{k\delta}(E_c, k - E_c, k - \omega) x U_{ck} + e_{vk} \mid U_{vk} \rangle \langle U_{ck} + e_{\beta q} \mid U_{ck} \rangle \quad (4.20)$$

Where Ω is the primitive cell volume, ω_k is the kpoint weight, U_{ck} is the periodic part of orbitals at the kpoint k, e_α is the unit vector in a cartisian coordinates. In addition v and c accounts for the valance band and conduction band states. The

imaginary part is used to obtain the real part of dielectrics function by using the kramers kroning transformation as following

$$\varepsilon^{(1)}_{\alpha\beta}(\omega) = 1 + \frac{2p}{\pi}\int_0^\infty \frac{\varepsilon^{(2)}_{\alpha\beta}(\omega')(\omega)d\omega'}{\omega'^2 - \omega^2} \tag{4.21}$$

where p is the principal value.

Light normally incident on a solid will be partially reflected at the air (or vacuum) and solid interface, and the remaining light will enter the solid. If it is absorbed by the solid, its intensity will decrease exponentially with distance as $e^{-\alpha(\lambda)x}$, where $\alpha(\lambda)$ is the absorption coefficient. The energy levels of systems can have a variety of mechanisms by which electrons (and holes) absorb optical energy. Most of these processes can occur in quantum wells, wires, and dots, as well as in bulk material.

Band-to-band: an electron in the valence band absorbs a photon with enough energy to be excited to the conduction band, leaving a hole behind.

Band-to-exciton: an electron in the valence band absorbs almost enough energy to be excited to the conduction band. The electron and hole it leaves behind remain electrically "bound" together, much like the electron and proton of a hydrogen atom. As we see from figure 4.8 while increasing the external hydrostatic pressure the absorption cofficient of the material increases and reached highest peak at a minimum photon energy.

The peak is obesrved at 1eV corresponds mainly to the transitions either from the occupied O(p) to unoccupied states of conduction bands.

These findings are in broad agreement with the experimental results, calculated at ambient pressure.

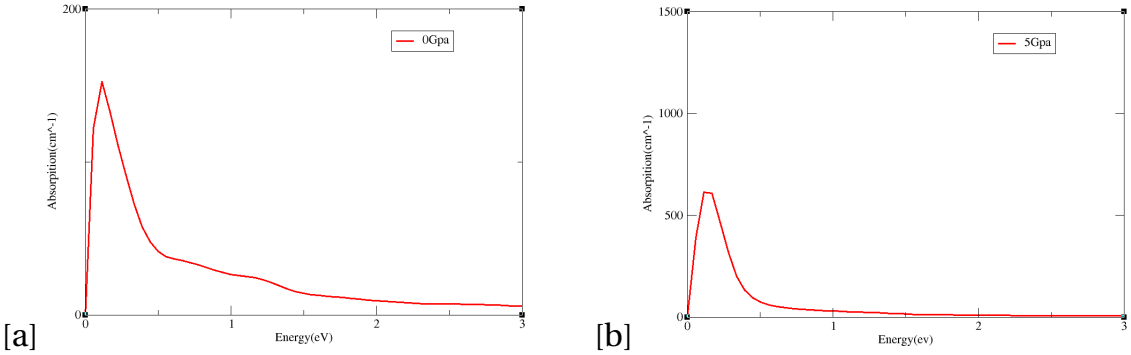

Fig. 4.9: Figure a) and b) represents absorption cofficient versus photon energy subjected to various external hydrostatic pressure respectively.

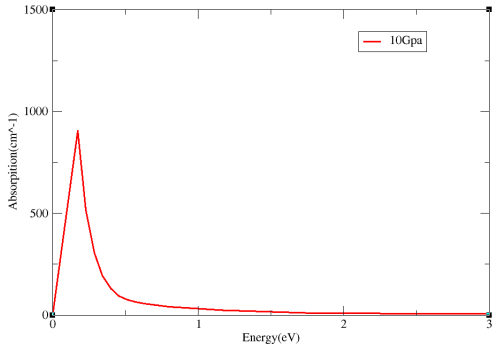

Fig. 4.10: Figure represents absorption cofficient versus photon energy at 10Gp.

4.7 effect of Pressure on structural and electronic properties of BiFeO_3

Figure 4.11 shows the perspective views of the BiFeO_3 structure. It contains six Bi atoms, six Fe atoms and eighteen O atoms, each Bi atom is surrounded by six O atoms and each Fe atoms, are surrounded by six O atoms. The nearest neighbor $<Fe-O>$ distances are 2.44693Å, $<Bi-Fe>$ distances are 1.6Å, and $<Bi-O>$ distances are 2.6608Å which are excellent in agreement with the experimental value. The experimental and optimized structure of BiFeO_3 has approximately similar structure as the system has not made shift in a phase transition. But while we have a good observation at these two structures the optimized structure is more re-

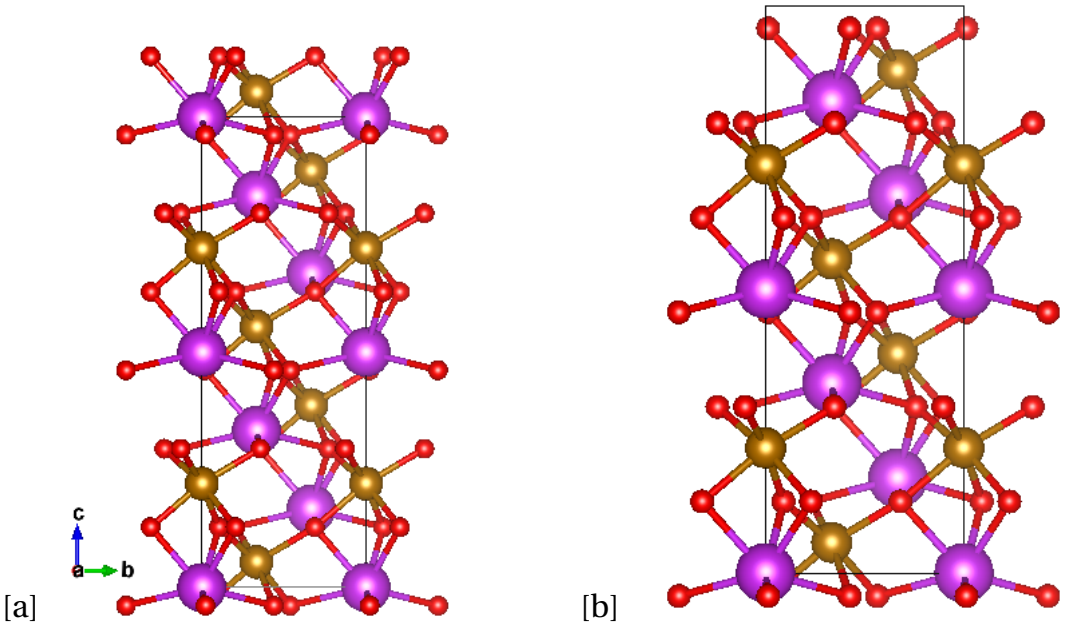

[a] [b]

Fig. 4.11: Figure a) and b) represents experimental and optimized structure of BiFeO_3 respectively.

laxed than the experimental one.

After geometry optimization, we have calculated pressure of BiFeO_3 by varing the experimental lattice parameter. The unit cell volume (V) of BiFeO_3 is 372.92Å and then plotted as a function of pressure(P). From figure 4.12(a) we have observed that the volume decreases with increasing pressure. And the calculated values of energy, E for this structure as a function of volume (V) is also shown in figure 4.12(b).

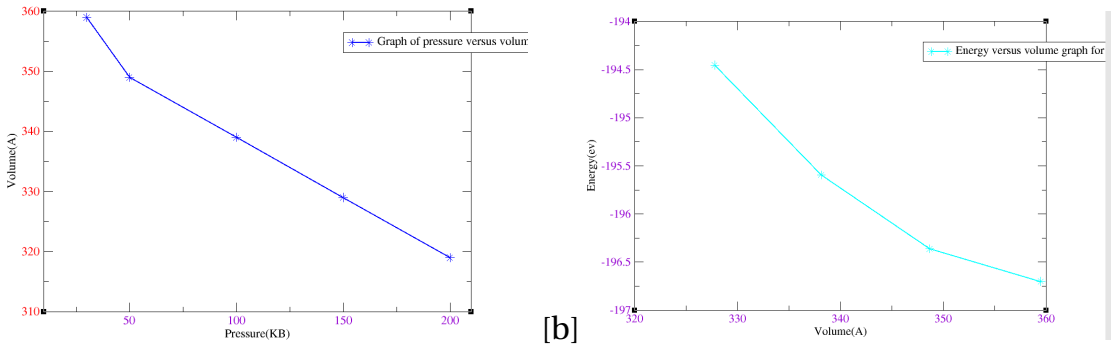

h [a] [b]

Fig. 4.12: Figure a and b represents pressure and energy versus volume graphs of $BiFeO_3$ respectively.

h [a] 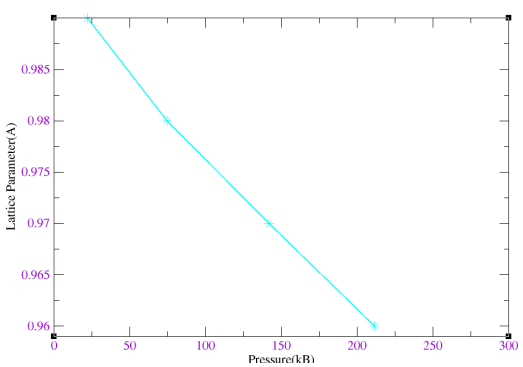

[b] 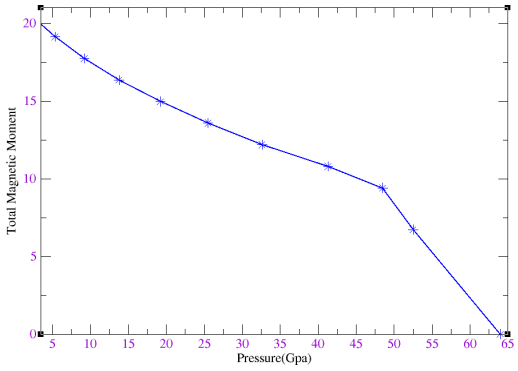

Fig. 4.13: Figure a and b represents lattice parameter and total magnetic moment versus Pressure graphs.

The pressure dependence of the lattice parameters of this compound is plotted in figure 4.13(a). The variation of the lattice parameter with pressure clearly shows the anisotropy in bonding of the compound.

From figure 4.13(b) it can be seen that as pressure is increasing total magnetic moment of the system drops down. This means that while the Pressure increases slightly from 2Gpa to 45Gpa the total magnetic moment of system decreases steadly. On the otherhand while the Pressure is in the range of 45Gpa to 63Gpa magnetization decreases rapidly and reaches to zoro at 64Gpa. While the pressure is increasing beyound this value the magnetic order parameter will change into another magnetic order state. These results are in good agreement with the available theoretical and experimental data.

We have performed a systematic investigation of $BiFeO_3$ under the hydrostatic pressure up to 65 GPa, while keeping the a/c ratio as constant throughout the calculations. We have compared our results relating to the angles of $BiFeO_3$ with the existing experiments. At ambient condition (0GPa), we have found the values of Bi-Fe-O3 = 89.98. The variation of these angles as a function of the applied hydrostatic pressure has been shown in figure 4.14, where we have seen that the angles decrease

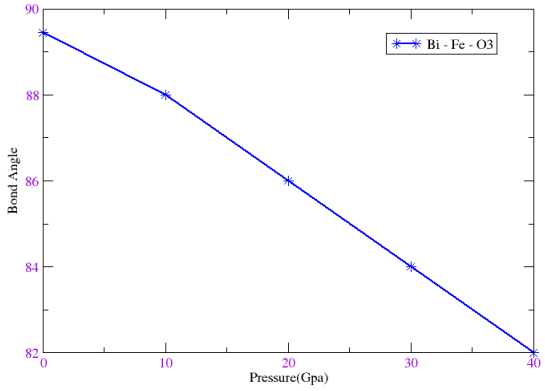

Fig. 4.14: Variation with pressure of some characteristic angles around a cation site of $BiFeO_3$

with increasing pressure.

5

High Pressure driven Superconducting critical temperature in Iron based Superconductors(SmAsFeOF)

Superconductivity, the mysterious absence of electrical resistance and appearance of complete diamagnetism manifesting in some materials below a critical temperature, has drawn a lot of attention from physicists since its first identification by Kamerlingh Onnes and his colleagues of Leiden University, the Netherlands in 1911. Due to its great potential in the technology of electrical engineering, information, track transportation, bio medicine, the research of superconductivity has always been an attractive field in science. In particular, high temperature(HT) superconductivity, which appears above the temperature of McMillan Limit (commonly assumed as 39k) under ambient pressure, has been assiduously explored by scientists all over the world.

The use of superconductors in magnets is limited by the fact that strong magnetic fields above a certain critical value, depending upon the material, cause a superconductor to revert to its normal, or non superconducting, state, even though the material is kept well below the transition temperature. Suggested uses for superconducting materials include medical magnetic imaging devices, magnetic energy

storage systems, motors, generators, transformers, computer parts, and very sensitive devices for measuring magnetic fields, voltages, or currents. The main advantages of devices made from superconductors are low power dissipation, high speed operation, and high sensitivity [59]. Most superconducting elements have been found to become superconducting at low temperatures. However, frequently it is necessary to apply pressure.

Superconductors are characterized not only by the absence of electrical resistance. They were furthermore found to exhibit certain unusual properties [60]. Most notably among those is the Meissner effect (exclusion of magnetic field from) [61]. A superconductor is a perfect diamagnet (a magnetic field is completely expelled from its bulk. However, for one kind of superconductors, usually called type-I superconductors, there is a critical field H_c above which the superconductivity is destroyed and the magnetic field can penetrate the material. There are also type-II superconductors for them there exists a lower critical field H_{c1} above which the magnetic flux lines can penetrate the bulk of the superconductor with out destroying the superconductivity and an upper critical field H_{c2} above which the superconductivity is destroyed [62]. Another striking property of superconductors.

From the beginning superconductivity attracted large efforts from theoretical physicists. But the first successful step on the way to a microscopic understanding of superconductivity was not made before 1950 when quantized lattice vibrations(phonons) were realized [63], which, can lead to an attractive effective interaction between electrons in a metal. Bardeen, Cooper and Schrieffer developed BCS theory of superconductivity in 1957 [64] which could describe all superconductors known at that time. The BCS theory is based on the idea that electrons in a shell of width of the Debye frequency around the Fermi surface can overcome the Coulomb

repulsion via the exchange of virtual phonons leading to an effective attractive interaction. Due to this interaction two electrons with opposite spin and momentum form bound pairs (usually called Cooper pairs) which then build up a superconducting phase coherent condensate. This new state of matter is characterized by the gap function or order parameter. The gap function is non zero in the vicinity of the Fermi surface only, where, with in the original BCS theory, it is isotropic and finite.

Interaction between superconductivity and magnetism has always been an area of interest in condensed matter physics, especially because of the antagonistic nature of these two phenomena. In a superconductor, the electron pairs, called Cooper pairs, are formed by electrons of opposite spin, which cancels the pairs. When the material is placed in a strong magneticfield, the spins are forced to orient themselves along the field. Usually, this breaks the pairs and destroys superconductivity. The magnetic fields inside a magnetically ordered material tend to act in the same manner, and thus superconductivity and magnetism tend to avoid each other. This mechanism is in agreement with the suppression of superconductivity due to exchange scattering between the superconducting electron and the local moments [65]. It has generally been believed that, within the context of the BCS theory of superconductivity, the conduction electrons in a metal can not be both ferromagnetically ordered and superconducting.

The recent observation of superconductivity at 56K in rare earth system, **SmAsFeOF** [66, 67] has marked the discovery of the first non copper oxide based high temperature magnetic superconductor. To date, all families of Fe based systems exhibit a clear evidence of superconductivity, with the highest transition temperatures up to 55K-56K in the 1111 family, [68]. Therefore FebSC is the second family of high

temperature superconductors.

In this section, we are reporting the change of superconducting critical temperature in Iron based Superconductivity **SmAsFeOF** under the influence of an external hydrostatic pressure based on first principles electronic structure calculations coupled with Migdal Eliashberg model [69,70]. Experimentally, it was shown previously that **SmAsFeOF** was undergoing a transition to a superconducting phase when subjected to a compressive pressure.

All the calculations are performed using the first principle pseudopotential method in the framework of density functional theory (DFT) with generalized gradient approximation as implemented in the VASP code.

We have used 8x8x2 Gamma point grid, a plane wave basis set cut off energy of 800eV and default generalized gradient approximation (GGA) density function (DF). In VASP code, we have used the ultrasoft pseudopotential for **SmAsFeOF**. As the name suggests, ultrasoft pseudopotential attain much smoother pseudo wave functions.

It has been observed that a number of TIs undergo a transition to a superconducting state with an external pressure or by intercalation with element like copper(Cu) [71–74]. This opens up an enormous possibility of investigations and applications of TIs. The hidden mechanism that leads to the superconducting phase and the corresponding essential factors that are responsible for the increase of T_c , with respect to the external pressure, should be envisaged extensively in order to have the possible applications of topological superconductors. It is worth mentioning that the Cu intercalation study of Bi_2Se_3 suggests the alternate possibility of superconductivity rather than the electron phonon coupling [75]. Our results suggest that the electron phonon coupling is the possible relevant mechanism for the

superconductivity, with the corresponding density of state (DOS) at the Fermi level increasing up to the external pressure of 30 GPa. For pressure greater than 30GPa, a decrease in DOS at the Fermi level has been observed leading to the decrement of the critical temperature in this material.

The structural and electronic properties have been investigated based on Density Functional Theory (DFT), as implemented in the Quantum Espresso and Vasp package [76].

12x12x3 k-points mesh is used to calculate the electron phonon interaction. The electron phonon coupling constant is given by Migdal Eliashberg theory [77] as follows:

$$\lambda = 2\int_0^\infty \omega^{-1}(\alpha)^2 F(\omega) d\omega \tag{5.1}$$

Where the integrand of the above is the Eliashberg spectral function.

$$\alpha^2 F(\omega) = \frac{1}{2}\sum_v \int \frac{1}{\pi N(f)} \frac{\alpha_q v}{\omega_{qv}} \gamma(\omega - \omega) \tag{5.2}$$

Considering λ as the electron phonon coupling constant and $\mu*$ as the reduced Coulomb repulsion, the critical temperature is then calculated using Allen Dynes formula

$$T_c = \frac{\omega_{log}}{1.2} exp(\frac{-1.04(1+\lambda)}{\lambda(1-0.62\mu*) - \mu*}) \tag{5.3}$$

Where ω is the phonon frequency. In this work, we have used $\mu* = 0.1$. The ω_{log} is defined as

$$\omega_{log} = exp[\frac{2}{\lambda}\int \frac{\alpha^2 F(\omega) log\omega}{\omega} d\omega] \tag{5.4}$$

Fig. 5.1 shows the variation of the density of states (DOS) with respect to the hydrostatic pressure exerted on **SmAsFeOF** . The system initially shows a band gap of 0.83eV in the absence of any external applied pressure. However, with the increasing external pressure, the energy gap is decreasing and the system has be-

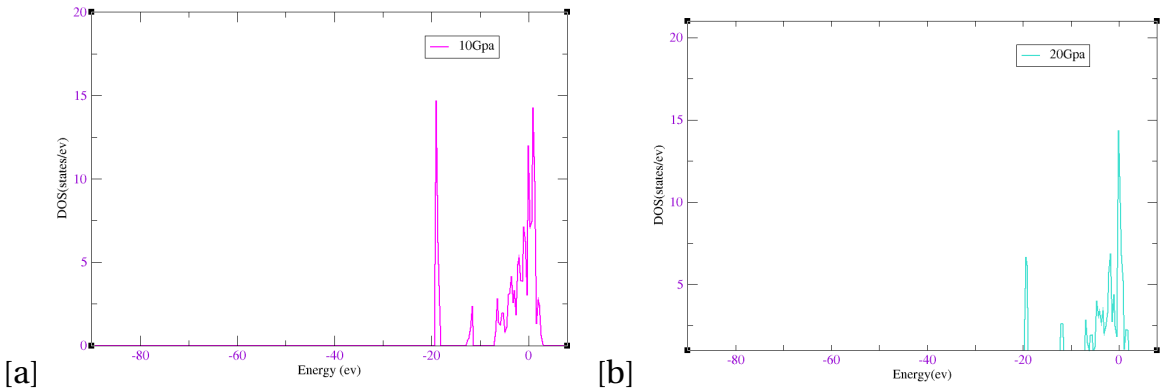

[a] [b]

Fig. 5.1: Total(a) and partial(b) density of states as a function of energy subjected to various external pressure.

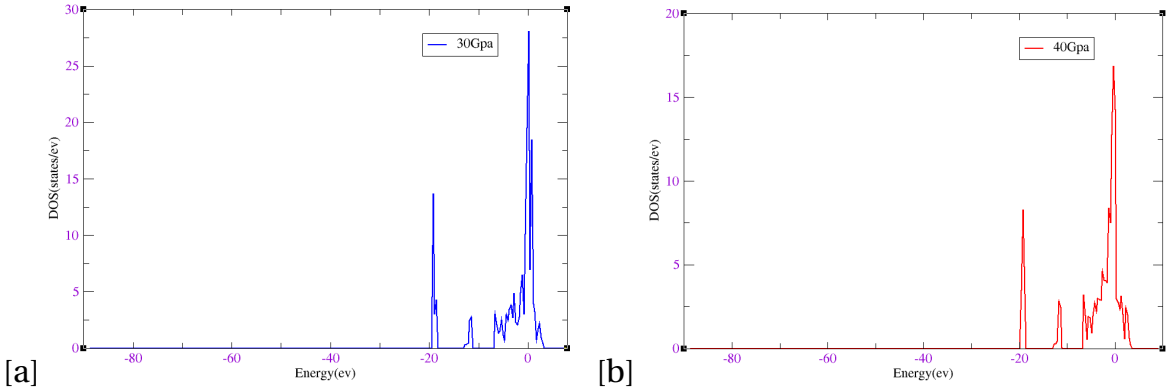

[a] [b]

Fig. 5.2: Total(a) and partial(b) density of states as a function of energy subjected to various external pressure.

come gapless at 10GPa. Therefore, 10GPa is designated as the transition pressure for semiconducting to metal transformation in **SmAsFeOF** system. If one goes on increasing the pressure, it has been found that above 0GPa, the DOS increases significantly with sharp peaks near the vicinity of the Fermi level. We also found the existence of superconducting phase for pressure greater than 10GPa.

The evolution of the phonon density of states (PHDOS) with increasing hydrostatic pressure for **SmAsFeOF** is demonstrated in Figure(5.1-5.3). This observation is in reasonable agreement with already reported theoretical work.

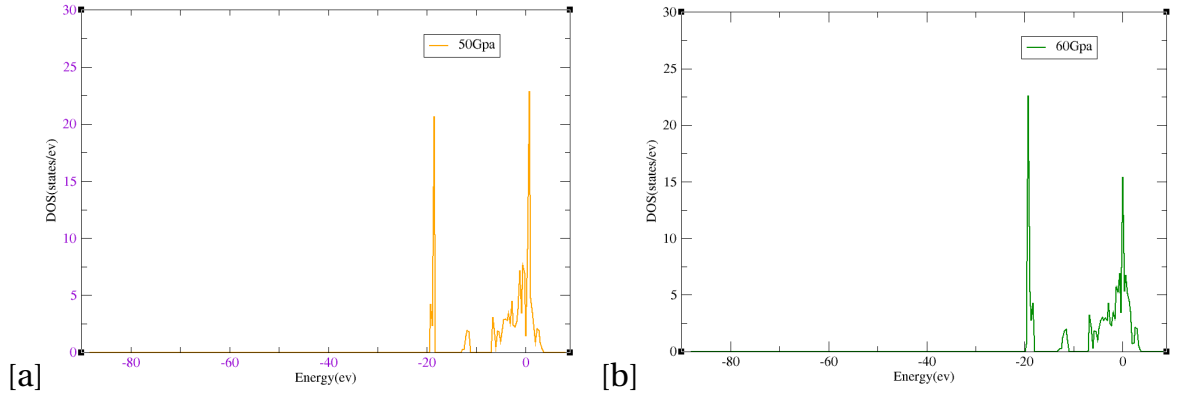

Fig. 5.3: Total(a) and partial(b) density of states as a function of energy subjected to various external pressure.

As a subsequent study of the above, we have undertaken the investigation to estimate the superconducting critical temperature (T_c) as a function of pressure using the Migdal Eliashberg theory coupled with first principles based calculations. This theory is based on the assumption that the Cooper pairs are formed mainly due to a phonon induced interaction between the fermions. All the relevant parameters in this theory such as the electron phonon coupling constant (λ), the electronic density of states at the Fermi energy $N(f)$, the Eliashberg spectral function $(\alpha)^2F(\omega)$, and the reduced Coulomb repulsion ($\mu*$) are determined in order to find the final value of T_c . Figure 5.4(a) shows the variation of estimated T_c as a function of pressure. A monotonically increasing value of T_c with the increasing pressure has been observed until 30GPa, and after that, T_c has dropped down with the exerternal pressure up to 60GPa. This variation profile of T_c with the hydrostatic pressure is closely correlated with corresponding variation of electron phonon coupling constant(λ), value. The maximum value that the critical temperature has reached is 45.91K at 30GPa, which is approximately 10.09 K less as compared to the experimental value of $SmFeFOAS$. The variation of T_c with pressure and variation of λ with pressure has been shown in Fig. 5.4(b) and Fig. 5.5 respectively, which is revealing a direct

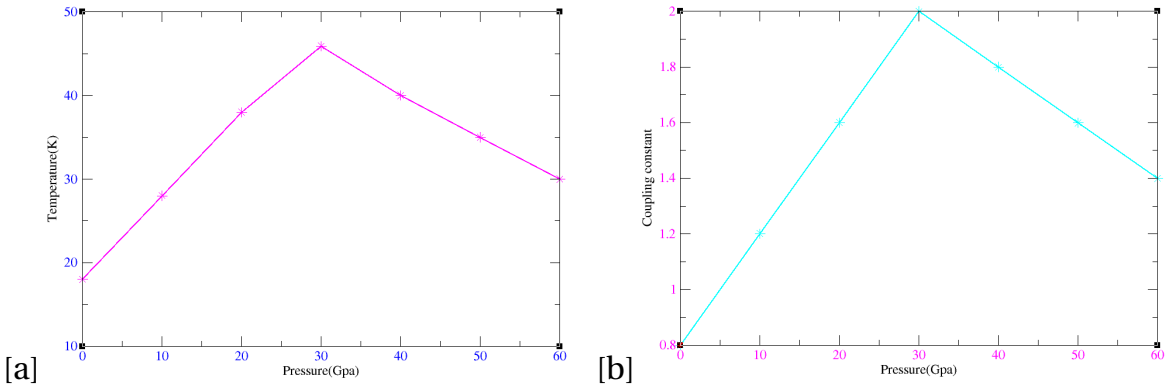

Fig. 5.4: Figure a and b represents estimation of temperature T(k) and coupling constant as a function of pressure respectively.

relationship between these two quantities.

The corresponding critical temperature T_c shows a monotically increase up to 30Gpa. The value of T_c has dropped with increasing of pressure above 30Gpa and, we have observed this decrement up to 60Gpa consistently.

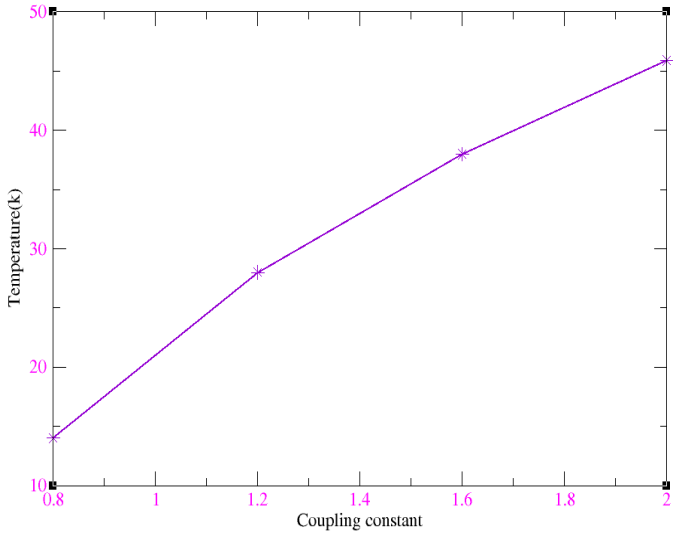

Fig. 5.5: Variation of temperature T(k) with coupling constant subjected to various external hydrostatic pressure.

From figure 5.5 we have seen that the critical temperature of $SmFeFOAs$ increases up to 45.91k under the coupling constant up to $\lambda = 2$, in the presence of external hydrostatic pressure.

6

Results and Discussions

We have described the manipulation of the magnetization of , ferrromagnetic multiferroic materials by external electric field. We have also examined role of magnetic field, electric field, and coupling term on spin density wave, magnetization, internal energy, and specific heat capacity of system. Using the model Hamiltonian and retarded double time temperature dependent Green's function formalism, we have obtained the expressions for reduced magnetization, dispersion relation, magnetic susceptibility, and specific heat capacity of system.

We studied the spin wave ω_k versus wave vector k at various EEF, which is shown in Figure 3.1. As seen in this figure, when the EEF increases the spin wave dispersion is affected, with the appearance of the gap.

Based on Eq.(3.50) we plotted the M(T) versus T(k) at various EEF. The magnetization increases as electric field increases, resulting in the enhancement of critical temperature T_c.

Magnetization versus electric field is also plotted in Fig.3.3 at various magnetic field, based on Eq(3.50). The magnetization increases as the magnetic field increases as expected. In figure 3.4 we study the behaviour magnetic susceptibility by changing the EEF, leading to enhancement of magnetic order, will have an effect on the ferroelectricity. Figure 3.5 represents variation of specific heat capacity with

temperature subjected to various EEF. As the field increases specific heat capacity of system also increases.

In the second section we have used the first principle theory to study the electronic and structural properties of $BiFeO_3$ and iron based superconductor($SmAsFeOF$). If one goes on increasing the pressure of $BiFeO_3$, the DOS decrease slightly near the vicinity of the fermi level as shown in figure(4.2-4.7).

From figure 4.11, we found the experimental and optimized structure of $BiFeO_3$ which has approximately similar structure as the system has not made shift in a phase transition. But optimized structure is more relaxed than the experimental one.

From figure 4.13(b) we have seen that total magnetic moment of the system drops down as pressure increases. Which means while the Pressure increases slightly from 2Gpa to 45Gpa the total magnetic moment of system decreases steadly, whihle pressure increases above this value magnetic moment decrease rapidly, then shifts to other magnetic order.

We also estimated dielectric and optical properties of $BiFeO_3$ at equilibrum lattice constants are calculated on the basis of calculated electronic structure for the energy range up to 3eV. The absorpition spectrum and optical energy is presented in figure 4.8-4.9. We found that the absorpitive part of dielectric function showed one peak, correspondigly to the electronic transition between occupied states and unoccupied states. The highest peak is observed at 0.1eV, corresponds to mainly to transitions, either occupied O(p) to Bi(d) unoccupied states of conduction band.

We have performed a systematic investigation of **SmAsFeOF** system under pres-

sure up to 60GPa, while keeping the a/c ratio as constant throughout the calculations. If one goes on increasing the pressure, it has been found that above 10GPa, the DOS increases significantly with sharp peaks near the vicinity of the Fermi level. Figure. 5.1-5.3 shows the variation of estimated T_c as a function of pressure. A monotonically increasing value of T_c with the increasing pressure has been observed until 30GPa, and after that, T_c has dropped down with the exerted pressure up to 60GPa. The maximum value that the critical temperature has attained is 45.91k at 30 GPa, which is approximately 10k less as compared to the experimental value of **SmAsFeOF** .

7

Conclusions

We have studied electric field induced and enhanced magnetic properties of multiferroic materials, and other properties of these materials. Using a model Hamiltonian and Green's function formalism we obtained expressions for reduced magnetization, dispersion relation, magnetic susceptibility , specific heat capacity system. Based on these mathematical expressions we plotted the graphs of m(T) vs T, ω_k vs k, C(T) vs T,$\chi_M(T)$ vs T at various EEF. We also plotted M(T) vs E at various magnetic field(B), keeping the temperature constant.

We also studied electronic and structural properties of multiferroic material($BiFeO_3$) and iron based superconductor($SmAsFeOF$) using the density functional theory applying Vasp and Quantum Espersso code.

The results of our work are described:

A) As EEF and B increase magnetization increases resulting in the enhancement of the critical temperature T_c.

B) Dispersion creates energy gap develops at non zero fields.

C) As EEF increases specific heat capacity also increases until it reaches a saturation.

D) At large value of external hydrostatic pressure of $BiFeO_3$, the DOS decrease slightly near the vicinity of the fermi level, leading to decrease total magnetic moment of system.

E) As external hydrostatic pressure of $SmAsFeOF$ increases, the DOS increases significantly with sharp peaks near the vicinity of the Fermi level, leads to increase electron phonon coupling constant(λ), Hence, the critical temperature of $SmFeFOAs$ increases up to 45.91k at 30Gpa pressure.

F) The value of T_c has dropped with incrasing pressure above 30Gpa, and we have observed this decrement upto 60Gpa consistently.

The results are in broad agreement with experiments.

Bibliography

[1] *G. A. Smolenskii and V. A. Bokov, Coexistence of Magnetic and Electric Ordering in Crystals, Journal of Applied Physics, Vol. 35, No. 3, 1964.*

[2] J. Mater. Chem.,17, 4931-4938, 2007.

[3] *D. Khomskii, Trend: Classifying Multiferroics: Mechanisms and Effects, Physics, Vol. 2, No. 20, 2009.*

[4] Randrianarivony, M. Erratum to On DFT Molecular Simulation for Non-Adaptive Kernel Approximation [Advances in Materials Physics and Chemistry 105-115] Advances in Materials Physics and Chemistry, 5, 95-95.Vol. 4 No. 6 (June 2014)

[5] *H. Schmid, Some Symmetry Aspects of Ferroics and Single Phase Multiferroics, Journal of Physics: Condensed Matter, Vol. 20, No.43,2008.*

[6] A. K.Singh, D. Jain, V.Ganesa, A. K. Nigam and S.Patnaik,Field-Dependent Competing Magnetic Ordering in Multiferroic Ni3V2O8, EPL,Vol. 86, No. 5, 2009.

[7] *J.-I. Igarashi and T. Nagao, Analysis of Optical Magnetoelectric Effect in GaFeO3,Physical Review B, Vol. 80, No. 5, 2009.*

[8] J. H. Lee, et al., A Strong Ferroelectric Ferromagnet Created by Means of Spin-Lattice Coupling,Nature, Vol.466, 2010.

[9] *D. N. Astrov, J. Exp. Theoret. Phys. (U.S.S.R) 38, 948 (1960).*

[10] V. J. Folen, G. T. Rado, and E. W. Stader, Phys. Rev. Lett. 6,607 (1961).

[11] *G. T. Rado and V. J. Folen, Phys. Rev. Lett. 7, 310 (1961).*

[12] A. K. Agyei and J. L. Birman, J. Phys. Condens. Matt. 2, 3007-3020 (1990).

[13] *S. W. Cheong and M. Mostovoy. Multiferroics: a magnetic twist for ferroelectricity. Nat. Mater., 6:1320, 2007.*

[14] Igor Levin, Jianhua Li, Julia Slutsker, and Alexander L. Roytburd, Adv. Mater., 18,20442047 (2006).

[15] *R. Ramesh and N. A. Spaldin. Multiferroics: progress and prospects in thinfilms. Nat. Mater., 6:2129, 2007.*

[16] H. Mueller. Properties of rochelle salt. iii. Phys. Rev., 58:565 573, 1940.

[17] *H. Mueller. Properties of rochelle salt. iv. Phys. Rev., 58:805811, 1940.*

[18] J. C. Slater. Theory of the transition of KH 2 PO 4 . J. Chem. Phys., 9:1633,1941.

[19] *B. M. Wul and I. M. Goldman. Dielectric constants of titanates of metals of the second group. Dokl. Akad. Nauk SSSR, 46:154157, 1945.*

[20] C. Kittel, Introduction to Solid State Physics, 8th ed.,(John Wiley and Sons,USA(2005)).

[21] *C. Tian, C. Lee, H. Xiang, Y. Zhang, C. Payen, S. Jobic, and M.-H. Whangbo.Magnetic structure and ferroelectric polarization of MnWO 4 investigated by density functional calculations and classical spin analysis. Phys. Rev. B, 80:104426, Sep 2009.*

[22] Spaldin N A 2005 Science 309 391.

[23] *Wang K F, Liu J M and Ren Z F 2009 Adv. Phys.*

[24] Spaldin N A, Cheong S W and Ramesh R Phys. Today 63 38. 2010

[25] *T. Katsufuji, H. Takagi, Phys. Rev. B 64 (2001).*

[26] J.F. Scott, Phys. Rev. B 16 (1977).

[27] *G. Lawes, A.P. Ramirez, C.M. Varma, M.A. Subramanian, Phys. Rev. Lett. 91(2003).*

[28] Scott J F 2012 J. Mater. Chem. 22 4567.

[29] *N. A. Hill, J. Phys. Chem. B 104, 6694 (2000).*

[30] D. I. Khomskii, Bull. Am. Phys. Soc. C 21.002 (2001).

[31] *J. Wang et al., Science 299 (5613), 1719-1722 (2003).*

[32] T. Kimura et al., Nature, 426, 55-58 (2003).

[33] *N. Hur et al., Nature 429, 392-395 (2004).*

[34] Hans Schmid, J. Phys.: Condens. Matter 20 434201(2008).

[35] *W. Eerenstein, N. Mathur, and J.F. Scott, Nature 442, 759 (2006).*

[36] V.V. Shvartsman, S. Bedanta, P. Borisov, W. Kleemann, A. Tkach and P. M. Vilarinho, Phys.Rev. Lett. 101, 165704 (2008).

[37] *D. N.Astrov, Sov. Phys. JETP 11, 708 (1960).*

[38] L.D. Landau and E.M. Lifshitz, Electrodynamics of Continuous Media (1960).

[39] *Cheong S W and Mostovoy M 2007 Nat. Mater. 6 13.*

[40] Wesselinowa J M and Kovachev S 2007 J. Appl. Phys. 102 043911

[41] *Gao X S, Liu J M, Chen X Y and Liu Z G 2000 J. Appl. Phys. 88 4250*

[42] Bahoosh S G, Wesselinowa J M and Trimper S 2013 Phys.

[43] *Bahoosh S G and Wesselinowa J M 2013 .*

[44] URL http://apps.webofknowledge.com/.

[45] *J. Valasek. Piezoelectric and allied phenomena in rochelle salt. Phys. Rev., 17:475481, 1921.*

[46] C. Piermarocchi, pochung chen, L. J. Sham, and D. G. Steel, Phys. Rev. Lett.89, 167402 (2002).

[47] *A. S. Chakravarty, 1980, Introduction to the Magnetic properties of solids, (John Wiley Son, Calcutta, India).*

[48] D. N. Zubarev, Sov. Phys. Usp. 3, 320 (1960).

[49] *M. Fiebig, J. Phys. D, Appl. Phys. 38, R123 (2005).*

[50] N.A. Hill, J. Phys. Chem. B 104, 6694 (2000).

[51] *G. Catalan, J.F. Scott, Adv. Mater. 21, 2463 (2009).*

[52] J.F. Scott, J. Magn. Magn. Mater. 321, 1689 (2009).

[53] *Song G L, Luo Y P, Su J, Zhou X H and Chang F G 2013 Acta Phys.Sin. 62 97502 (in Chinese).*

[54] Fundamentals and applications of density functional theory.mp4.

[55] *R.M.Martin, Cambridge University Press(2004).*

[56] I.R. Shein, V.V. Bannikov, A.L. Ivanovskii, Physica C 468 (2008) 1.

[57] *D. Vanderbilt, Phys. Rev. B 41, 7892 (1990).*

[58] Kresse, G. and Furthmller, J., Efficient iterative schemes for ab initio total-energy calculations using a plane-wave basis set. Physical Review B, 1996.

[59] *H. Kamerlingh Onnes, Comm. Phys. Lab. Univ. Leiden, Nos. 119, 120, 122 (1911).*

[60] J. R. Schrieffer, Theory of Superconductivity, Westview Press, Boulder, 1999; M. Tinkham, Introduction to Superconductivity, Dover Books on Physics, New York, 2004.

[61] *A. A. Abrikosov, Rev. Mod. Phys. 76, 975 (2004).*

[62] M. Kugler et al., Rev. Mod. Phys. 79, 353 (2007).

[63] *J. Bardeen, Phys. Rev. 106, 162 (1957); , Phys. Rev., 108, 1175 (1957).*

[64] B. T. Matthias et al . ,Phys. Rev. Lett. 1, 92 (1958).

[65] *A. A. Abrikosov, and L. P. Gorkov, Zh. Eksp. Teor. Fiz. 39, 1781 (1960).*

[66] A. Partrick et al., Rev. Mod. Phys. 78, 1 (2006).

[67] *H. H. Wen et al., Euro. Phys. Lett. 82, 17009 (2008).*

[68] R. Prozorov et al., J. Phys 449, 012020 (2013).

[69] *A. B. Migdal, Sov. Phys. JETP 34, 996 (1958).*

[70] G. M. Eliashberg, Sov. Phys. JETP 11, 696 (1960).

[71] *J. Zhu, J. L. Zhang, P. P. Kong, S. J. Zhang, X. H. Yu, J. L. Zhu, Q. Q. Liu, X. Li, R. C. Yu, R. Ahuja, W. G. Yang, G. Y. Shen, H. K. Mao, H. M. Weng, X. Dai, Z. Fang, Y. S. Zhao, and C. Q. Jin, Sci. Rep. 3, 2016 (2013).*

[72] T. V. Bay, T. Naka, Y. K. Huang, H. Luigjes, M. S. Golden, and A. de Visser, Phys. Rev. Lett. 108, 057001 (2012).

[73] *S. Sasaki, M. Kriener, K. Segawa, K. Yada, Y. Tanaka, M. Sato, and Y. Ando, Phys. Rev. Lett. 107, 217001 (2011).*

[74] M. Kriener, K. Segawa, Z. Ren, S. Sasaki, and Y. Ando, Phys. Rev. Lett.106, 127004 (2011).

[75] *X.-L. Zhang and W.-M. Liu, Sci. Rep. 5, 8964 (2015).*

[76] P. Giannozzi, S. Baroni, N. Bonini, M. Calandra, R. Car, C. Cavazzoni, D. Ceresoli, G. L. Chiarotti, M. Cococcioni, I. Dabo et al., J. Phys.: Condens. Matter 21, 395502 (2009).

[77] *G. M. Eliashberg, Sov. Phys. JETP 11, 696 (1960).*

[78] W. Kohn and L. J. Sham. Self-consistent equations including exchange and correlation effects. Phys. Rev., 140:A1133A1138, Nov 1965.

[79] *M. Fuchs, M. Bockstedte, E. Pehlke, and M. Scheffler. Pseudopotential study of binding properties of solids within generalized gradient approximations: The role of core-valence exchange correlation. Phys. Rev. B, 57:21342145, Jan 1998.*

[80] John P. Perdew, Robert G. Parr, Mel Levy, and Jose L. Balduz. Density-functional theory for fractional particle number: Derivative discontinuities of the energy. Phys. Rev. Lett., 49:16911694, Dec 1982.

[81] *B. Hammer, L. B. Hansen, and J. K. Nrskov Phys. Rev. B 59, 7413 Published 15 March 1999.*

[82] ACTA PHYSICA POLONICA A Vol. 117 page 182 (2010)